reprogramming mechanisms. Further published work with this technique is eagerly anticipated, as several questions have still to be answered: for example what cells are being transduced to generate these iPS cells? Can this be done with human cells? What is the molecular basis of reprogramming induced by the four factors? Is it the same process that happens during NT and cell fusion reprogramming? Can the implicated genes be activated and induce reprogramming without use of oncogenic virus (Surani, 2007)?

Screening for reprogramming factors

Reprogramming remains largely phenomenological, and efforts should now aim to dissect the mechanism at the molecular level (Hochedlinger and Jaenisch, 2006). Oocytes, preimplantation embryos, and pluripotent stem cells contain factors sufficient for reprogramming, and so constitute good material for identifying reprogramming factors (Hamatani *et al.*, 2004; Ko, 2006). Beyhan *et al.* (2007) reported global gene expression analysis of bovine NT, IVF embryos and donor somatic cells to characterize differences in their transcription profiles. They have found a small set of genes differentially expressed as well as genes of donor cells persistently expressed in NT embryos. Investigating gene expression changes that occur during or soon after reprogramming should elucidate the molecular mechanisms involved.

Another approach includes the use of mass spectrometry to identify reprogramming factors in cells and cell-derived extracts (Koziol *et al.*, 2007). Cell extracts have been shown to induce transient changes in gene expression and chromatin structure in differentiated cells (Dimitrov and Wolffe, 1996), which, if maintained, could possibly result in reprogramming. However, a caveat to these approaches is that the initial induction of reprogramming may only involve subtle changes in gene expression that then cumulatively elicit a pronounced effect. A more forceful approach would be to individually overexpress the four factors shown by Yamanaka and colleagues to reprogram differentiated cells (Takahashi and Yamanaka, 2006) and analyse the resulting genome-wide changes in gene expression. Alternatively, small molecule or RNAi screens could be performed to identify the important factors (Edwards, 2006).

Induction and maintenance of nuclear programmes has, for many years, been considered to be directed solely by proteins involved in gene regulation and morphogenic signalling. Many researchers have carried out reprogramming screens for proteins only to pull out generic chromatin remodeling factors. Additional candidates now need to be considered, including non-proteinaceous macromolecules. RNA, for example, has now emerged as a key player in a surprisingly large number of gene regulation studies. For example, the activity of X chromosomes in female mammals is controlled by non-coding RNAs such as *Xist* and *Tsix*. Furthermore, microRNAs (miRNAs), a large family of short non-coding RNAs (17–25 nucleotides) that mainly function to repress expression of their target genes, regulate blood development (Yekta *et al.* 2004). Tang *et al.* (2007) have recently showed a large proportion of the maternal genes are directly or indirectly under the control of miRNAs, which demonstrates that the maternal miRNAs are essential for the earliest stages of mouse embryonic development. It would not be surprising if non-coding RNA has further roles in specific and stable regulation of developmental programmes. miRNA may have an important role in nuclear reprogramming.

An alternative approach to studying artificial reprogramming, which could be expanded further, has been to study naturally induced reprogramming in lower vertebrates where it occurs successfully and more frequently and to look for common elements in more complex organisms. Unlike mammals, many fish and amphibia have the capacity to regenerate complex structures such as limbs after injury. Even mammals have this capacity in Msx1 expressing regions at the digit termini and more widely during early embryonic phases (Han *et al.*, 2003). This process involves cell migration and a change in cell phenotype in response to the injury. There are certain caveats here, however. It is hard to dissect process important for reprogramming from other processes such as the innate immune response, cell migration, and other consequences of injury. It is also unknown to what extent these processes are conserved in mammals. Still, dedifferentiation of cells to form proliferating progenitor cells is interesting, and systems such as skeletal muscle, limb and tail regeneration or dorsal iris epithelium during lens regeneration should be studied further with screens designed to find the key players involved.

The main challenge facing elucidation of nuclear reprogramming mechanisms using the conventional approaches, and potential solutions

The main problem with current studies investigating nuclear reprogramming mechanisms is the lack of material due to the low frequencies of reprogramming using artificial methods. Conventional approaches entail isolating and expanding reprogrammed cells in strongly selective culture conditions [e.g. in cell fusion experiments (Tada *et al.*, 1997; Cowan *et al.*, 2005) hybrid clones were isolated by antibiotic resistance and expanded]. Analysing such material, however, does not allow discrimination between the epigenetic changes necessary for the induction of reprogramming versus those that happen independently of such induction; i.e. it does not allow the study of reprogramming as it is happening.

How can the study of this process be facilitated? One strategy is to use easily reprogrammable cells, such as cells differentiated from ES cells in culture (Blelloch *et al.*, 2006; Silva *et al.*, 2006). Perhaps the initial focus should be on cultured cells instead of later primary cells, as these will still have strong epigenetic regulation, and thus would be harder to reprogram. Experiments with cultured cells should yield more reprogrammed material.

Additionally, it would be possible to use chromatin modifying drugs such as trichostatin A and 5-aza-2'-deoxycytidine to make the chromatin less condensed and more accessible. Factors required for activating the *Oct-3/4* gene are unknown, but recently it has been shown that two chromatin modifying drugs can activate the *Oct-3/4* gene in cells (Hattori *et al.*, 2004). These two drugs, trichostatin A (TSA) and 5-aza-2'-deoxycytidine

(5-aza-dC), which inhibit histone deacetylation and DNA methylation respectively, are thought to make the chromatin structure more open and consequently the *Oct-3/4* gene easier to activate. However, such drug treatment is quite toxic to the cells as well as being non-specific (these drugs reactivate many genes including those not associated with an ES cell phenotype (S Sullivan, unpublished data). Tsuji-Takayama *et al.* (2004) have recently shown that treatment of differentiated ES cells with a similar chemical to 5-aza-dC, called 5-azacytidine, causes the up-regulation of stem cell marker genes *Oct-3/4*, *Nanog* and *Sox2*. As with Hattori's work, the expression of genes associated with differentiated cells were not studied, and it is expected that these too will be up-regulated. It will be very interesting to screen for more specific drugs that increase the frequency of reprogramming.

Thirdly, although the reason is unknown, cell cycle synchronization by serum starvation makes murine embryonic fibroblasts (MEF) more easily reprogrammed both by NT (Campbell, 1996) or cell fusion (Sullivan *et al.*, 2006) This strategy could also facilitate reprogramming studies.

Can one learn about reprogramming and improve its efficiency by transposing conditions between the three reprogramming methods?

In order to learn from experiments using the three different methods to deduce the reprogramming mechanism(s) and improve their efficiencies, it is necessary to compare and contrast observations from them. At present, it is difficult to dissect the important events such as changes in gene regulation and chromatin structure during the reprogramming processes due to the inefficiency of all three methods, but some hints can be gathered from existing kinetic, gene expression, and cell cycle data. The kinetics of reprogramming appears to be very similar between NT and cell fusion. Somatic cell-derived transgenic Oct-3/4 is expressed within 24 h after NT and cell fusion (Sullivan and Egli, unpublished data). In contrast, reprogramming experiments using viral transduction have shown that stem cell genes *Alkaline Phosphatase*, *SSEA-1*, and *Nanog* are not highly expressed until 2–3 weeks post-infection (Blelloch *et al.*, 2007; Maherali *et al.* 2007; Meissner *et al.* 2007; Okita *et al.* 2007; Wernig *et al.* 2007), indicating that reprogramming proceeds at a slower pace with this method. The need to synthesize the four reprogramming genes *de novo* can only partially explain the slower kinetics of reprogramming using the viral transduction method. It is likely that other proteins that facilitate the induction of reprogramming during NT and cell fusion are missing, or that the entire transcriptional programme required for reprogramming, which is more completely expressed by the oocyte during NT or the ES cell during cell fusion, is vast and requires a substantial amount of time to execute. For example, demethylation of promoters of endogenous genes such as Oct-3/4 may occur very slowly during reprogramming by viral transduction if factors required for active demethylation are not produced as they are thought to be during NT (Yamazaki *et al.* 2006).

The two pluripotency genes used in the iPS cell viral transduction approach, *Oct-3/4* and *Sox2*, are expressed in oocytes (Avilion *et al.*, 2003; Monti *et al.*, 2006) and mouse ES cells (Yamanaka, 2007), suggesting that their roles in establishing and/or maintaining pluripotency are conserved in all three reprogramming approaches. Yamanaka posits that c-Myc may make the chromatin more accessible to transcription factors by binding to many sites in the genome and inducing histone deacetylation in addition to promoting self-renewal, as it does in murine ES cells (Cartwright *et al.* 2005; Yamanaka, 2007). c-Myc is expressed in oocytes (Naz *et al.* 1994) but is not highly expressed in mouse ES cells (Blelloch *et al.*, 2007). However, a functionally equivalent family member, n-Myc, is expressed and can substitute for c-Myc in iPS cell transduction (Blelloch *et al.*, 2007). Thus, Myc proteins may stimulate self-renewal in iPS cell transduction, cell fusion and NT. *Klf-4* is highly expressed in mouse ES cells (Yamanaka, 2007) and thus may play a role in reprogramming during cell fusion.

Cell cycle synchronization of the somatic cells into G_0/G_1 or G_2/M prior to NT or cell fusion increases the efficiency of reprogramming (Campbell *et al.*, 1996; Sullivan *et al.*, 2006). This effect is attributable to avoiding the aneuploidy or chromosomal damage risked by nuclear transfer or cell fusion during S phase. Yamanaka used unsynchronized cells in the iPS cell transduction experiments because active cell division is a requirement for infection by Moloney retrovirus. Egli and coworkers determined that a zygote arrested in mitosis can reprogram a somatic nucleus while an interphase zygote cannot (Egli *et al.*, 2007). A major difference between a mitotic zygote and an interphase zygote is that the nuclear membrane has broken down in the mitotic zygote. Therefore, it is possible that factors required for reprogramming are sequestered in the nucleus during interphase and released during mitosis. In cell fusion in mice, ES cells in G_2/M phase were the most effective at reprogramming, suggesting that key reprogramming activities at that stage of the cell cycle (Sullivan *et al.*, 2006).

Now there is the opportunity to use observations made in one method of reprogramming to try to improve the other methods. For example, will overexpressing some or all of the four Yamanaka factors in ES cells make reprogramming by cell fusion more efficient? The best evidence that this might be the case is given by Silva and coworkers. They reported elevated frequencies of reprogramming in a cell fusion system where *Nanog*, a pluripotency gene not necessary for iPS cell formation by viral transduction, was overexpressed in the ES cell fusion partner (Silva *et al.*, 2006). High Nanog levels may assist the induction of reprogramming indirectly as positive feedback circuits involving Nanog elevate Oct-3/4 and Sox2 levels (Loh *et al.*, 2006).

It will also be interesting to introduce c-*Myc* and *Klf-4* transgenically into cells to be reprogrammed by NT or cell fusion, to see if this increases the frequency of reprogramming; however, as these gene are both oncogenes, the resultant cells should be tested for epigenetic and genetic abnormalities. There is an additional caveat with this approach; what is learned from reprogramming genetically manipulated, cultured cells may not immediately inform the process of reprogramming normal primary somatic cells, which still have all epigenetic regulatory processes intact. It is, however, a first step towards reprogramming primary cells and should give enough material to untangle the various mechanisms.

Slow demethylation or chromatin re-structuring may be why Yamanaka's viral transduction method proceeds more slowly than NT or cell fusion. This seems likely, given that the other two methods have other factors that could potentially speed up these processes. For example, Yamazaki and coworkers found that even in NT, demethylation of the *Oct-4* promoter proceeds gradually and is probably a result of both active and passive mechanisms for demethylation (Yamazaki *et al.*, 2006). Yamanaka's four factors may not be sufficient to induce active demethylation, and may be dependent on the passive mechanism alone, causing slower reprogramming. Overexpression of de-novo methyl-transferase genes such as *Dnmt-1* or *Dnmt-3* might facilitate the process. Alternatively, if chromatin remodelling is the rate-limiting step, small molecule HDAC inhibitors could expedite reprogramming.

In the future, determining the list of genes that are up-regulated in ES cells during G_2/M phase or proteins that are localized in the nucleus during interphase in zygotes will significantly concentrate the search for genes necessary for reprogramming. Additionally, Yamanaka's work suggests that transcription factor libraries may be the most fruitful source of reprogramming factors.

Currently, it seems reasonable that all three reprogramming methods share a general mechanism involving chromatin remodelling to allow changes in gene expression as the first step, followed by changes to prevent cell death. The last step would be the induction of pluripotency. It also seems likely that the genes used to induce pluripotency are the same in all three methods, while there could be different molecular pathways to cell immortalization and altering DNA accessibility.

Conclusion

NT is the only reprogramming technique known not to require addition of foreign genes to induce restoration of developmental potential. Furthermore, it is still the only method can restore pluripotency without a high risk of oncogenesis. Thus, NT remains a very important system for studying reprogramming. Efficiency by this and the other two methods discussed is, however, still very low and the lack of material limits efforts to identify important factors for reprogramming induction. All three methods (NT, cell fusion, and iPS cell transduction) should be perused so that conditions optimal in one system can be implemented in the others to try to improve reprogramming frequencies. The four iPS cell factors can be introduced into cells that are to be used in NT and cell fusion experiments with the hope of increasing the frequency of reprogramming. It is hoped this will provide more material to study mechanisms and so help understanding of reprogramming. The scarcity of tissues and organs for transplantation, as well as the need for pluripotent stem cells to develop in-vitro models of human disease and development, compel further study of reprogramming mechanisms.

Acknowledgements

SS is funded by a fellowship from the Harvard Stem Cell Research Foundation. JI is funded by a fellowship from the New York Stem Cell Foundation. AU and HA are funded by Health and Labour Sciences Research Grants, Japan. The authors thank Esther Son, Kit Rodolfa, Katelyn Foley, and Gabriella Boulting for proofreading the manuscript.

References

Avilion AA, Nicolis SK, Pevny LH *et al.* 2003 Multipotent cell lineages in early mouse development depend on SOX2 function. *Genes and Development* **17**, 126–140.

Baron MD, Kamata Y, Barras V *et al.* 1996 The genome sequence of the virulent Kabete 'O' strain of rinderpest virus: comparison with the derived vaccine. *Journal of General Virology* **77**, 3041–3046.

Barton SC, Arney KL, Shi W *et al.* 2001 Genome-wide methylation patterns in normal and uniparental early mouse embryos. *Human Molecular Genetics* **10**, 2983–2987.

Beyhan Z, Ross PJ, Iager AE *et al.* 2007 Transcriptional reprogramming of somatic cell nuclei during preimplantation development of cloned bovine embryos. *Developmental Biology* **305**, 637–649.

Blelloch R, Venere M, Yen J, Ramalho-Santos M 2007 Generation of induced pluripotent stem cells in the absence of drug selection. *Cell Stem Cell* **1**, 245–247.

Blelloch R, Wang Z, Meissner A *et al.* 2006 Reprogramming efficiency following somatic cell nuclear transfer is influenced by the differentiation and methylation state of the donor nucleus. *Stem Cells* **24**, 2007–2013.

Boshart M, Nitsch D, Schutz G 1993 Extinction of gene expression in somatic cell hybrids – a reflection of important regulatory mechanisms? *Trends in Genetics* **9**, 240–245.

Brambrink T, Hochedlinger K, Bell G, Jaenisch R 2006 ES cells derived from cloned and fertilized blastocysts are transcriptionally and functionally indistinguishable. *Proceedings of the National Academy of Sciences of the USA* **103**, 933–938.

Briggs R, King TJ 1952 Transplantation of living nuclei from blastula cells into enucleated frogs' eggs. *Proceedings of the National Academy of Sciences of the USA* **38**, 455–463.

Broyles RH 1999 Use of somatic cell fusion to reprogram globin genes. *Seminars in Cell and Developmental Biology* **10**, 259–265.

Campbell KH 1999 Nuclear equivalence, nuclear transfer, and the cell cycle. *Cloning* **1**, 3–15.

Campbell KH, Loi P, Otaegui PJ, Wilmut I 1996 Cell cycle co-ordination in embryo cloning by nuclear transfer. *Reviews of Reproduction* **1**, 40–46.

Cartwright P, McLean C, Sheppard A *et al.* 2005 LIF/STAT3 controls ES cell self-renewal and pluripotency by a Myc dependent mechanism. *Development* **132**, 885–896.

Cibelli JB, Stice SL, Golueke PJ *et al.* 1998 Cloned transgenic calves produced from nonquiescent fetal fibroblasts. *Science* **280**, 1256–1258.

Counter CM, Avilion AA, LeFeuvre CE *et al.* 1992 Telomere shortening associated with chromosome instability is arrested in immortal cells which express telomerase activity. *EMBO Journal* **11**, 1921–1929.

Cowan CA, Atienza J, Melton DA, Eggan K 2005 Nuclear reprogramming of somatic cells after fusion with human embryonic stem cells. *Science* **309**, 1369–1373.

Davidson RL 1974 Gene expression in somatic cell hybrids. *Annual Review of Genetics* **8**, 195–218.

Di Giorgio FP, Carrasco MA, Siao MC *et al.* 2007 Non-cell autonomous effect of glia on motor neurons in an embryonic stem cell-based ALS model. *Nature Neuroscience* **10**, 608–614.

Dimitrov S, Wolffe AP 1996 Remodeling somatic nuclei in *Xenopus laevis* egg extracts: molecular mechanisms for the selective release of histones H1 and H1(0) from chromatin and the acquisition of transcriptional competence. *EMBO Journal* **15**, 5897–5906.

Edwards RG 2006 Genetics, epigenetics and gene silencing in differentiating mammalian embryos. *Reproductive BioMedicine Online* **13** 732–753.

Eggan K, Akutsu H, Loring J *et al.* 2001 Hybrid vigor, fetal overgrowth, and viability of mice derived by nuclear cloning and tetraploid embryo complementation. *Proceedings of the National*

Academy of Sciences of the USA **98**, 6209–6214.
Egli D, Rosains J, Birkhoff G, Eggan K. 2007 Developmental reprogramming after chromosome transfer into mitotic mouse zygotes. *Nature* **447**, 679–685.
Evans MJ, Kaufman MH 1981 Establishment in culture of pluripotential cells from mouse embryos. *Nature* **292**, 154–156.
Fulka J Jr, First NL, Moor RM 1996 Nuclear transplantation in mammals: remodelling of transplanted nuclei under the influence of maturation promoting factor. *Bioessays* **18**, 835–840.
Gridelli B, Remuzzi G 2000 Strategies for making more organs available for transplantation. *New England Journal of Medicine* **343**, 404–410.
Gurdon JB 1968 Nucleic acid synthesis in embryos and its bearing on cell differentiation. *Journal of Embryology and Experimental Morphology* **20**, 401–414.
Gurdon JB, ElsdaleTR, Fischberg M. 1958 Sexually mature individuals of *Xenopus laevis* from the transplantation of single somatic nuclei. *Nature* **182**, 64–65.
Hakelien AM, Landsverk HB, Robl JM *et al.* 2002 Reprogramming fibroblasts to express T-cell functions using cell extracts. *Nature Biotechnology* **20**, 460–466.
Hamatani T, Carter GM, Sharov AA *et al.* 2004 Dynamics of global gene expression changes during mouse preimplantation development. *Developmental Cell* **6**, 117–131.
Han M, Yang X, Farrington JE, Muneoka K 2003 Digit regeneration is regulated by Msx1 and BMP4 in fetal mice. *Development* **130**, 5123–5132.
Hattori N, Nishino K, Ko Y *et al.* 2004 Epigenetic control of mouse Oct-3/4 gene expression in embryonic stem cells and trophoblast stem cells. *Journal of Biological Chemistry* **279**, 17063–17069.
Hochedlinger K, Jaenisch R 2006 Nuclear reprogramming and pluripotency. *Nature* **441**, 1061–1067.
Hochedlinger K, Jaenisch R 2002 Nuclear transplantation: lessons from frogs and mice. *Current Opinion in Cell Biology* **14**, 741–748.
Kass SU, Wolffe AP 1998 DNA methylation, nucleosomes and the inheritance of chromatin structure and function. *Novartis Foundation Symposium* **214**, 36–50.
Kato K, Gurdon JB 1993 Single-cell transplantation determines the time when *Xenopus* muscle precursor cells acquire a capacity for autonomous differentiation. *Proceedings of the National Academy of Sciences of the USA* **90**, 1310–1314.
Kato Y, Tani T, Sotomaru Y *et al.* 1998 Eight calves cloned from somatic cells of a single adult. *Science* **282**, 2095–2098.
Kelly SJ 1977 Studies of the developmental potential of 4- and 8-cell stage mouse blastomeres. *Journal of Experimental Zoology* **200**, 365–376.
Kikyo N, Wade PA, Guschin D *et al.* 2000 Active remodeling of somatic nuclei in egg cytoplasm by the nucleosomal ATPase ISWI. *Science* **289**, 2360–2362.
Ko SHM 2006 Expression profiling of the mouse early embryo: reflections and perspectives. *Developmental Dynamics* **235**, 2437–2448.
Koziol MJ, Garrett N, Gurdon JB 2007 Tpt1 activates transcription of Oct3/4 and nanog in transplanted somatic nuclei. *Current Biology* **17**, 801–807.
Lindsey J, McGill NI, Lindsey LA, Green *et al.* 1991 In-vivo loss of telomeric repeats with age in humans. *Mutation Research* **256**, 45–48.
Loh YH, Wu Q, Chew JL *et al.* 2006 The Oct4 and Nanog transcription network regulates pluripotency in mouse embryonic stem cells. *Nature Genetics* **38**, 431–440.
Maherali N, Sridharan R, Xie W *et al.* 2007 Global epigenetic remodeling in directly reprogrammed fibroblasts. *Cell Stem Cell* **1**, 55–70.
Martinez-Balbas MA, Dey A, Rabindran SK *et al.* 1995 Displacement of sequence-specific transcription factors from mitotic chromatin. *Cell* **83**, 29–38.
Matsui YK, Zsebo K Hogan BL 1992 Derivation of pluripotential embryonic stem cells from murine primordial germ cells in culture. *Cell* **70**, 841–847.
McGrath J, Solter D 1984 Inability of mouse blastomere nuclei transferred to enucleated zygotes to support development in vitro. *Science* **226**, 1317–1319.
Meissner A, Jaenisch R 2006 Mammalian nuclear transfer. *Developmental Dynamics* **235**, 2460–2469.
Meissner A, Wernig M, Jaenisch R 2007 Direct reprogramming of genetically unmodified fibroblasts into pluripotent stem cells. *Nature Biotechnology* **25**, 1177–1181.
Monk M, Boubelik M, Lehnert S 1987 Temporal and regional changes in DNA methylation in the embryonic, extraembryonic and germ cell lineages during mouse embryo development. *Development* **99**, 371–382.
Monti M, Garagna S, Redi C, Zuccotti M 2006 Gonadotropins affect Oct-4 gene expression during mouse oocyte growth. *Molecular Reproduction and Development* **73**, 685–691.
Naz RK, Kumar G, Minhas BS 1994 Expression and role of c-myc protooncogene in murine preimplantation embryonic development. *Journal of Assisted Reproduction and Genetics* **11**, 208–216.
Ogura A, Inoue K, Ogonuki N *et al.* 2000 Production male cloned mice fresh, cultured, and cryopreserved immature Sertoli cells. *Biology of Reproduction* **62**, 1579–1584.
Okita K, Ichisaka T, Yamanaka S 2007 Generation of germline-competent induced pluripotent stem cells. *Nature* **448**, 313–317.
Perreault SD 1992 Chromatin remodeling in mammalian zygotes. *Mutation Research* **296**, 43–55.
Peterson JA, Wess MC 1972 Expression of differentiated functions in hepatoma cell hybrids: induction of mouse albumin production in rat hepatoma-mouse fibroblast hybrids. *Proceedings of the National Academy of Sciences of the USA* **69**, 571–575.
Reik W, Kelsey G, Walter J 1999 Dissecting de novo methylation. *Nature Genetics* **23**, 380–382.
Resnick JL, Bixler LS, Cheng L, Donovan PJ 1992 Long-term proliferation of mouse primordial germ cells in culture. *Nature* **359**, 550-551.
Ribbert H 1911 *Das Karzinom des Menschen/Human Cancer*. Friedrich Cohen, Bonn.
Rideout WM 3rd, Eggan K, Jaenisch R 2001 Nuclear cloning and epigenetic reprogramming of the genome. *Science* **293**, 1093–1098.
Rodolfa KT, Eggan K 2006 A transcriptional logic for nuclear reprogramming. *Cell* **126**, 652–655.
Rodolfa K, Di Giorgio FP, Sullivan S 2007 Defined reprogramming: a vehicle for changing the differentiated state. *Differentiation* **75**, 577–579.
Schultz RM, Davis W Jr, Stein P *et al.* 1999 Reprogramming of gene expression during preimplantation development. *Journal of Experimental Zoology* **285**, 276–282.
Silva J, Chambers I, Pollard S, Smith A 2006 Nanog promotes transfer of pluripotency after cell fusion. *Nature* **441**, 997–1001.
Stojkovic M, Stojkovic P, Leary C *et al.* 2005 Derivation of a human blastocyst after heterologous nuclear transfer to donated oocytes. *Reproductive BioMedicine Online* **11**, 226–231.
Sullivan S, Eggan K 2007 The potential of cell fusion for human therapy. *Stem Cell Reviews* **2**, 341–350.
Sullivan S, Pells S, Hooper M *et al.* 2006 Nuclear reprogramming of somatic cells by embryonic stem cells is affected by cell cycle stage. *Cloning Stem Cells* **8**, 174–188.
Surani MA 2007 Afterword. In: Sullivan S, Chad CA, Eggan K (eds) *Human Embryonic Stem Cells: The Practical Handbook*, John Wiley and Sons, Ltd, Chichester, UK, 389–391.
Surani MA 1999 Reprogramming a somatic nucleus by trans-modification activity in germ cells. *Seminars in Cell and Developmental Biology* **10**, 273–277.
Tada M, Takahama Y, Abe K *et al.* 2001 Nuclear reprogramming of somatic cells by in vitro hybridization with ES cells. *Current Biology* **11**, 1553–1558.
Tada M, Tada T, Lefebvre L *et al.* 1997 Embryonic germ cells induce epigenetic reprogramming of somatic nucleus in hybrid cells. *EMBO Journal* **16**, 6510–6520.
Takahashi K, Yamanaka S 2006 Induction of pluripotent stem cells from mouse embryonic and adult fibroblast cultures by defined

factors. *Cell* **126**, 663–676.

Tang F, Kaneda M, OCarroll D *et al.* 2007 Maternal microRNAs are essential for mouse zygotic development. *Genes and Development* **21**, 644–648.

Tsuji-Takayama K, Inoue T, Ijiri Y *et al.* 2004 Demethylating agent, 5-azacytidine, reverses differentiation of embryonic stem cells. *Biochemical and Biophysical Research Communications* **323**, 86–90.

Vaziri H, West MD, Allsopp RC *et al.* 1997 ATM-dependent telomere loss in aging human diploid fibroblasts and DNA damage lead to the post-translational activation of p53 protein involving poly(ADP-ribose) polymerase. *EMBO Journal* **16**, 18–33.

Verlinsky Y, Strelchenko N, Kukharenko V *et al.* 2005 Human embryonic stem cell lines with genetic disorders. *Reproductive BioMedicine Online* **10**, 105–110.

Wakayama T, Tabar V, Rodriguez I *et al.* 2001 Differentiation of embryonic stem cell lines generated from adult somatic cells by nuclear transfer. *Science* **292**, 740–743.

Wakayama T, Tateno H, Mombaerts P, Yanagimachi R 2000 Nuclear transfer into mouse zygotes. *Nature Genetics* **24**, 108–109.

Wakayama T, Perry AC, Zuccotti M *et al.* 1998 Full-term development of mice from enucleated oocytes injected with cumulus cell nuclei. *Nature* **394**, 369–374.

Weismann A 1893 The Germ-Plasm: A Theory of Heredity. Charles Scribner's Sons, New York.

Weiss MC, Chaplain M 1971 Expression of differentiated functions in hepatoma cell hybrids: reappearance of tyrosine aminotransferase inducibility after the loss of chromosomes. *Proceedings of the National Academy of Sciences of the USA* **68**, 3026–3030.

Wernig M, Meissner A, Foreman R *et al.* 2007 In vitro reprogramming of fibroblasts into a pluripotent ES-cell-like state. *Nature* **448**, 318–324.

Willadsen SM 1986 Nuclear transplantation in sheep embryos. *Nature* **320**, 63–65.

Wilmut I, Schnieke AE, McWhir J *et al.* 1997 Viable offspring derived from fetal and adult mammalian cells. *Nature* **385**, 810–813.

Wobus AM, Boheler KR 2005 Embryonic stem cells: prospects for developmental biology and cell therapy. *Physiological Reviews* **85**, 635–678.

Wright WE, Brasiskyte D, Piatyszek MA, Shay JW 1996 Experimental elongation of telomeres extends the lifespan of immortal x normal cell hybrids. *EMBO Journal* **15**, 1734–1741.

Yamanaka S 2007 Strategies and new developments in the generation of patient-specific pluripotent stem cells. *Cell Stem Cell* **1**, 39–44.

Yamazaki Y, Fujita TC, Low EW *et al.* 2006 Gradual DNA demethylation of the Oct4 promoter in cloned mouse embryos. *Molecular Reproduction and Development* **73**, 180–188.

Yekta S, Shih IH, Bartel DP. 2004 MicroRNA-directed cleavage of HOXB8 mRNA. *Science* **304**, 594–596.

Received 27 July 2007; refereed 12 September 2007; accepted 17 October 2007.

STEM CELLS
TISSUE-SPECIFIC STEM CELLS

Novel Cardiac Precursor-Like Cells from Human Menstrual Blood-Derived Mesenchymal Cells

NAOKO HIDA,[a,b,c] NOBUHIRO NISHIYAMA,[a,c] SHUNICHIRO MIYOSHI,[a,d] SHINICHIRO KIRA,[a] KAORU SEGAWA,[e] TARO UYAMA,[b] TAISUKE MORI,[c] KENJI MIYADO,[b] YUKINORI IKEGAMI,[a,b] CHANGHAO CUI,[b] TOHRU KIYONO,[f] SATORU KYO,[g] TATSUYA SHIMIZU,[h] TERUO OKANO,[h] MICHIIE SAKAMOTO,[c] SATOSHI OGAWA,[a] AKIHIRO UMEZAWA[b]

[a]Department of Cardiology, Keio University School of Medicine, Tokyo, Japan; [b]Department of Reproductive Biology and Pathology, National Research Institute for Child Health and Development, Tokyo, Japan; [c]Department of Pathology, Keio University School of Medicine, Tokyo, Japan; [d]Institute for Advanced Cardiac Therapeutics, Keio University School of Medicine, Tokyo, Japan; [e]Department of Microbiology and Immunology, Keio University School of Medicine, Tokyo, Japan; [f]Virology Division, National Cancer Center Research Institute, Tokyo, Japan; [g]Department of Obstetrics and Gynecology, Kanazawa University, School of Medicine, Kanazawa, Japan; [h]Institute of Advanced Biomedical Engineering and Science, Tokyo Women's Medical University, Tokyo, Japan

Key Words. Cardiomyogenesis human mesenchymal stem cell • Menstrual blood endometrial gland • Cell sheet technology cardiac precursors

ABSTRACT

Stem cell therapy can help repair damaged heart tissue. Yet many of the suitable cells currently identified for human use are difficult to obtain and involve invasive procedures. In our search for novel stem cells with a higher cardiomyogenic potential than those available from bone marrow, we discovered that potent cardiac precursor-like cells can be harvested from human menstrual blood. This represents a new, noninvasive, and potent source of cardiac stem cell therapeutic material. We demonstrate that menstrual blood-derived mesenchymal cells (MMCs) began beating spontaneously after induction, exhibiting cardiomyocyte-specific action potentials. Cardiac troponin-I-positive cardiomyocytes accounted for 27%–32% of the MMCs in vitro. The MMCs proliferated, on average, 28 generations without affecting cardiomyogenic transdifferentiation ability, and expressed mRNA of GATA-4 before cardiomyogenic induction. Hypothesizing that the majority of cardiomyogenic cells in MMCs originated from detached uterine endometrial glands, we established monoclonal endometrial gland-derived mesenchymal cells (EMCs), 76%–97% of which transdifferentiated into cardiac cells in vitro. Both EMCs and MMCs were positive for CD29, CD105 and negative for CD34, CD45. EMCs engrafted onto a recipient's heart using a novel 3-dimensional EMC cell sheet manipulation transdifferentiated into cardiac tissue layer in vivo. Transplanted MMCs also significantly restored impaired cardiac function, decreasing the myocardial infarction (MI) area in the nude rat model, with tissue of MMC-derived cardiomyocytes observed in the MI area in vivo. Thus, MMCs appear to be a potential novel, easily accessible source of material for cardiac stem cell-based therapy. STEM CELLS *2008;26:1695–1704*

Disclosure of potential conflicts of interest is found at the end of this article.

INTRODUCTION

Marrow-derived mesenchymal stem cells (MSCs) are a potential cellular source for stem cell-based therapy, since they have the ability to differentiate into cardiomyocytes [1, 2], use of MSCs presents no ethical problems, and autologous MSCs have been injected into ischemic hearts clinically [3]. Direct injection of MSCs into the heart has been shown to be feasible in vivo [4–7], but with limited effect. The reason for this may be the extremely low rate of cardiomyogenesis exhibited by marrow-derived MSCs [2], with cardiac function improvement due to grafted MSC-induced neovascularization [7, 8] and an antiapoptotic

Author contributions: N.H.: conception and design, collection and assembly of data, data analysis and interpretation, final approval of manuscript; N.N.: conception and design, collection and assembly of data, data analysis and interpretation, manuscript writing, final approval of manuscript; S.M.: conception and design, administrative support, collection and assembly of data, data analysis and interpretation, manuscript writing, final approval of manuscript; S. Kira and Y.I.: collection and assembly of data, final approval of manuscript; K.S., C.C., T.K., S. Kyo, and T.S.: provision of study material, final approval of manuscript; T.U.: provision of study material, collection and assembly of data, final approval of manuscript; T.M.: collection and assembly of data, data analysis and interpretation, final approval of manuscript; K.M.: collection and assembly of data, final approval of manuscript; T.O.: administrative support, provision of study material, final approval of manuscript; M.S.: administrative support, final approval of manuscript; S.O.: financial support, administrative support, final approval of manuscript; A.U.: financial support, administrative support, manuscript writing, final approval of manuscript.

Correspondence: Shunichiro Miyoshi M.D., Ph.D., Keio University School of Medicine, 35-Shinanomachi, Shinjuku-ku, Tokyo, 160-8582 Japan. Telephone: +81-3-3353-1211 (ext 62310); Fax: +81-3-3353-2502; e-mail: smiyoshi@cpnet.med.keio.ac.jp Received October 2, 2007; accepted for publication April 6, 2008; first published online in STEM CELLS *EXPRESS* April 17, 2008. 1066-5099/2008/$30.00/0 doi: 10.1634/stemcells.2007-0826

effect on infarcted cardiomyocytes [9, 10]. To further improve prospects of restoring cardiac function, a search was initiated for another source of cells having high cardiomyogenic potential.

Our previous study showed that umbilical cord blood-derived mesenchymal stem cells (UCBMSCs) [11] and placental chorionic plate cells (PCPCs) [12] have a phenotype of mesenchymal cells and have higher cardiomyogenic differentiation ability in vitro. Since these materials are deemed medical waste and can be obtained without any ethical problems, they may be a suitable stem cell source for cardiac regenerative therapy. But the population of UCBMSCs in umbilical cord blood is scant [13] and there is also a problem in establishing PCPCs, since placental tissue contains a lot of maternal decidua-derived mesenchymal cells that could contaminate PCPCs. Therefore, it is difficult to obtain enough of these cells without using a limiting dilution method and/or massive ex vivo propagation, which may cause instability of the genome [14]. Consequently, material that contains a large amount of mesenchymal cells during the first few passages should be a highly suitable source of stem cells.

A previous paper suggests that endometrium contains an MSC-like population [15] and menstrual blood-derived mesenchymal (MMCs) cells have a pluripotent differentiation ability in vitro [16]. The data presented here demonstrate that human menstrual blood-derived mesenchymal cells and uterine endometrial gland-derived mesenchymal cells (EMCs) have a strong potential for cardiomyogenic transdifferentiation in vitro and in vivo. Moreover, large amounts of MMCs could be obtained from the first passage of menstrual blood culture, and MMCs have been shown to restore impaired cardiac function through marked cardiomyogenesis in vivo.

Materials and Methods

Isolation of MMCs and EMCs

After informed consent was obtained, mesenchymal cells from approximately 10 ml of menstrual blood of six women (20–30 years old) were collected on the first day of menstruation. The samples were suspended in Dulbecco's modified Eagle's medium (DMEM) high glucose supplemented with 10% FBS, and split into two 10-cm dishes. The estimated adherent cell number at the start of culture was approximately 1×10^7. The growth curve and phase-contrast microscopic view are shown in supplemental online Fig. 1. The results for MMCs obtained from six women were the same. A human endometrial tissue sample was also taken from a 52-year-old woman undergoing hysterectomy [17]. Individual endometrial glands were isolated under a microscope and then seeded. After the retroviral transfection of HPV16E6, E7, and hTERT [2], endometrial cell strains were generated by the limiting dilution method. Two strains exhibiting rapid cell division cycles were designated EMC100 and EMC214 (Fig. 3B and 3D, respectively). EMC100 and EMC214 showed adherent spindle shape morphology that proliferated for more than 250 population doublings without changing cardiomyogenic differentiation ability.

Isolation of Marrow-Derived Mesenchymal Stem Cells

Bone marrow-derived mesenchymal stem cells (BMMSCs) were obtained from a 41-year-old male as described previously [2].

Coculture with Murine Fetal Cardiomyocytes

MMCs, EMCs, and BMMSCs were infected with enhanced green fluorescent protein (EGFP) expressing adenovirus [2]. Fetal cardiomyocytes were obtained from hearts of day-17 mouse fetuses, as previously described [2]. The isolated cardiomyocytes were replated at $5 \times 10^4/cm^2$ on top of a floating athelocollagen membrane (CM-6, 40-μm thickness; Koken, Tokyo, http://www.kokenmpc.co.jp/english/products/collagen/cell_culture/cm-6_24/index.html) that is permeable for only small molecules (less than 5,000 MW). The next day, the athelocollagen membrane was plated upside down on the culture dish. Harvested EGFP-labeled MMCs and EMCs were then seeded upon the athelocollagen surface (bottom surface) at $7 \times 10^3/cm^2$ (Fig. 1M). In several experiments (Figs. 1G–1L, 2, 3E, 3H, 3K–3M, 4, supplemental online Fig. 2, examination of chromosome chimeras), we did not use the athelocollagen membrane for the coculture system.

Immunocytochemistry and Immunohistochemistry

A laser confocal microscope (FV1000; Olympus, Tokyo, http://www.olympus-global.com) was used for immunocytochemical analysis. Samples were stained with mouse monoclonal anti-cardiac troponin-I antibody (4T21 Lot 98/10-T21-C2; HyTest, Euro, Finland, http://www.hytest.fi/) or with mouse monoclonal anti-sarcomeric α-actinin antibody (Sigma-Aldrich, St. Louis, http://www.sigmaaldrich.com), or anti-connexin 43 antibody (Sigma-Aldrich) diluted 1:300 overnight at 4°C, then stained with TRITC-conjugated anti-mouse antibody (Sigma-Aldrich), TRITC-conjugated anti-rabbit antibody (Sigma-Aldrich), and Cy5-conjugated anti-mouse IgG (Chemicon, Temecula, CA, http://www.chemicon.com) diluted 1:100, containing 4′-6-diamidino-2-phenylindole (DAPI; Wako Chemical, Osaka, Japan, http://www.wako-chem.co.jp/english) at 1:300 for 30 minutes at 25°C–28°C. See also supplemental online data 1 for detail of method.

Functional Analysis

The method of action potential (AP) recording was as previously described [2] but with slight modification. A fluorescence inverted microscope (IX-70; Olympus) was used for AP recording. The microscope was equipped with a recording chamber and a noiseless heating plate (Microwarm Plate; Kitazato Supply, Fujinomiya, Shizuoka, Japan, http://www.kitazato-supply.com). A 10-mM volume of HEPES (Sigma-Aldrich) was added to the culture medium to stabilize the pH of the perfusate at 7.5. Standard glass microelectrodes having a direct current resistance of 15–25 MΩ when filled with pipette solution were used. Alexa 568 compound was dissolved to a concentration of 0.5 mM in 2 M of KCl solution in order to completely dissolve the Alexa 568 in the pipette solution. The electrodes were positioned with a motor-driven micromanipulator (PCS-5000; Burleigh Instrument, Inc., New York) under optical control. Spontaneously beating EGFP-positive cells were selected as targets, and after the APs of the target cells had been recorded, the dye was injected by iontophoresis (−7 nA for 10–20 seconds). The extent of dye transfer was monitored under a fluorescence microscope, and digital images were recorded with a digital photo camera (EOS-digital; Canon, Tokyo, http://www.canon.com) mounted on the microscope. The recording pipette was connected to a patch-clamp amplifier (MEZ-8300; Nihon Kohden, Tokyo, http://www.nihonkohden.com). The amplified signal was filtered with a 4-pole Bessel filter (NF-3625; NF electronic instrument; NF Corp., Tokyo, http://www.nfcorp.co.jp/english/index.html) set at 2 kHz, then digitized with an A/D converter with a sampling frequency of 10 kHz (Digidata 1,322A; Molecular Devices Corp., Union City, CA, http://www.moleculardevices.com). Pacemaker potential was defined by the slowly depolarizing membrane potential at phase IV of the AP.

Alexa 568 was injected into cells via recording microelectrodes to stain the cells and confirm that the AP was generated by EGFP-positive cells (Fig. 1G–1I, 3E, 3H). Since the dye did not diffuse into the EGFP-negative murine cardiomyocytes, there were no tight cell-to-cell heterologous connections (i.e., gap junctions), at least in the in vitro condition. In some experiments, Alexa 568 diffused into the EGFP-positive satellite EMCs and MMCs, suggesting that a homologous cell-to-cell connection had been established at least 1 week after cocultivation. The measured parameters of the APs were averaged and are shown in Figure 1K.

The fluorescent image of the beating MMCs and EMCs was monitored using a CCD camera (Ikegami Tsushin Co., Ltd, http://www.ikegami.co.jp) and was stored using digital video. The video images (National Television Standards Committee format, 29.97 frame/second) of contraction of EMCs and MMCs were stored in a personal computer as MPEG-2 format files, then analyzed later.

Both edges of the EGFP-positive EMCs and MMCs along the line (Figs. 1L, 3K) were automatically detected, and the distance between both edges was measured from each video frame using an image edge-detection program using Igor Pro 4 (Wavemetrics Inc., Lake Oswego, OR) [11].

Calculation of Induction Rate

The MMCs and EMCs were exposed to 3 μM 5-azacytidine (5-azaC; Sigma-Aldrich) for 24 hours to induce cell differentiation, or were left untreated. The 5-azaC-treated and nontreated MMCs or EMCs, cultivated with or without murine fetal cardiomyocytes, were enzymatically dissociated and stained, then observed by confocal laser microscope (supplemental online data 2 for detail of method). The cardiomyogenic induction rate (average of 10 separate experiments) was calculated as the fraction of cardiac troponin-I-positive cells in the EGFP-positive cells.

Examination of Chromosomes of MMCs or EMCs and Murine Cell Chimeras

To rule out cell fusion-dependent cardiomyogenesis, chromosomes from MMCs or EMCs cocultivated without separation by the athelocollagen membrane from murine cardiomyocytes for 1 week were stained using a human chromosome-specific probe and a mouse chromosome-specific probe (Chromosome Science Labo, Hokkaido, Japan, http://www.chromoscience.jp/en/probe/page01/page01e.html) and spectral karyotyping with fluorescent in situ hybridization chromosome painting technique (Applied Spectral Imaging, Vista, CA, http://www.spectral-imaging.com), according to the manufacturer's protocol.

RNA Extraction and RT-PCR

Reverse transcriptase polymerase chain reaction (RT-PCR) was done as described previously [2]. Primers for the following genes were used: cardiac transcription factors—Csx/Nkx-2.5 and GATA4; cardiac hormones—atrial natriuretic peptide and brain natriuretic peptide; cardiac structural proteins—cardiac troponin I, cardiac troponin T, myosin light chain-2a, myosin light chain-2v, and cardiac-actin; and ion channel—cyclic nucleotide-gated potassium channel 2 (supplemental online Table 1). The internal control was 18S rRNA. PCR primers were prepared such that they would amplify the human but not the mouse genes.

Flow Cytometric Analysis

The cells were analyzed using an EPICS ALTRA analyzer (Beckman Coulter, Fullerton, CA, http://www.beckmancoulter.com). Antibodies (anti-human CD10, CD13, CD14, CD24, CD29, CD31, CD34, CD44, CD45, CD54, CD55, CD59, CD71, CD73, CDw90, CD105, CD106, CD117, CD133, CD140a, CD166, CD309, HLA-ABC, and HLA-DR) [12] were purchased from Beckman Coulter, Immunotech (Luminy, France, http://www.beckmancoulter.com/products/pr_immunology.asp), Cytotech (Hellebaek, Denmark, http://www.cytotech.dk/index.html), Santa Cruz Biotechnology Inc. (Santa Cruz, CA, http://www.scbt.com), RDI (Research Diagnostics, Inc., Concord, MA, http://www.researchd.com), and Pharmingen Pharmaceutical, Inc. (San Diego, http://www.bdbiosciences.com/index_us.shtml).

In Vivo Cardiomyogenic Differentiation of EMCs

EGFP-labeled EMC tissue graft, made by a novel 3-dimensional cell sheet manipulation, was transplanted into male F344 nude rats (Clea, Tokyo, http://www.clea-japan.com/) (8 weeks of age). EMC100s and EMC214s ($2 \times 10^5/cm^2$) were plated onto fibrin polymer-coated culture dishes. Four days after plating, EMCs were detached as previously described [18], and transplanted onto the surface of the recipient heart (Fig. 5A) [19]. At 2 weeks after transplantation, immunohistochemical analysis was performed. EGFP-labeled EMC tissue graft on the fibrin polymer-coated culture dish did not show cardiomyogenic differentiation in vitro.

MMC Transplantation in Myocardial Infarction Model In Vivo

Recipient male F344 nude rats (Clea) (6 weeks of age) were anesthetized with 2% isoflurane gas. After left thoracotomy, the left ventricle was exposed and left anterior coronary artery was ligated by 6–0 silk suture. The complete occlusion of the coronary artery was confirmed by the cyanotic color and dyskinetic motion of the left ventricular anterior wall. In some rats, we did not ligate the coronary artery (Sham). The chest was closed and animals survived for 2 weeks to create complete myocardial infarction.

Two weeks after the first operation, rats with myocardial infarction were randomized for the control myocardial infarction (MI) group, the MI+BMMSC group, and the MI+MMC group, and were blinded immediately before the cell injection. Echocardiograms were performed on the anesthetized (2% isoflurane) rats. Data were collected three times and averaged. Immediately before transplantation, ~$1–2 \times 10^6$ of EGFP-positive MMC or BMMSC suspension was drawn up into a 50-μl Hamilton syringe (Hamilton Co., Reno, NV, http://www.hamiltoncompany.com/main_usa.asp) with a 31-gauge needle. A 10-μl portion of the cell suspension was injected into the center and margin of the infarcted myocardium (MI+MMC, Fig. 7A). In the control MI group, culture medium or ~$1–2 \times 10^6$ of murine cardiac fibroblast was injected. Immediately before cell transplantation, 2-dimensional and M-mode echocardiographic (8.5 MHz linear transducer, EnVisor C; Phillips Medical System, Andover, MA, http://www.medical.philips.com/index.html) images were obtained to assess left ventricular (LV) end-diastolic dimension and LV end-systolic dimension at the mid-papillary muscle level.

Two weeks after the transplantation, a similar echocardiogram was performed again; then after opening the abdomen, a blood sample was drawn from the abdominal great vein; then the left diaphragm was dissected to insert a 22-gauge manometer line into the left ventricle, which was connected to the transducer (model TP-400T; Nihon Kohden) to monitor left ventricular pressure. The electrocardiogram and measured pressure were digitized by PowerLabo (ADInstruments, Milford, MA, http://www.adinstruments.com) at the sample frequency of 10 KHz and stored in a personal computer (Macintosh iBook G4; Apple, Cupertino, CA, http://www.apple.com).

Tissue samples were obtained by fixing and slicing along the short axis of the left ventricle, for every 1-mm depth of the ventricle. After Masson's trichrome staining, digital images of samples were collected using a light microscope (IX-70; Olympus). The images were digitized and analyzed using an Igor Pro 4 (Wavemetrics Inc.). The pixel area of blue color (fibrosis area) was defined as the infarcted area, and the pixel area of red color was defined as "survived" myocardium. The data on each pixel area from each slice were collated and the percentage fibrosis area was calculated as follows: % Fibrosis = 100 × (Pixel area of blue color)/(Pixel area of blue color and red color).

Statistical Analysis

All data are shown as the mean value ± SE. The difference among mean values was determined with analysis of variance. The posthoc test (Bonferroni) was used when three or more groups were compared. Student's t test was used when two values were compared. Statistical significance was set at $p < .05$.

RESULTS

Cardiomyogenic Transdifferentiation of MMCs

To exclude cell fusion-dependent cardiomyogenesis [20], EGFP-labeled MMCs were cocultured in the same dish with mouse cardiomyocytes, separated by a 40-μm high-density athelocollagen membrane (Fig. 1M). The two cell types were never in direct contact. On day 5 after cocultivation commenced, approximately half of the MMCs were beating strongly in a synchronized manner (supplemental online Video 1). Im-

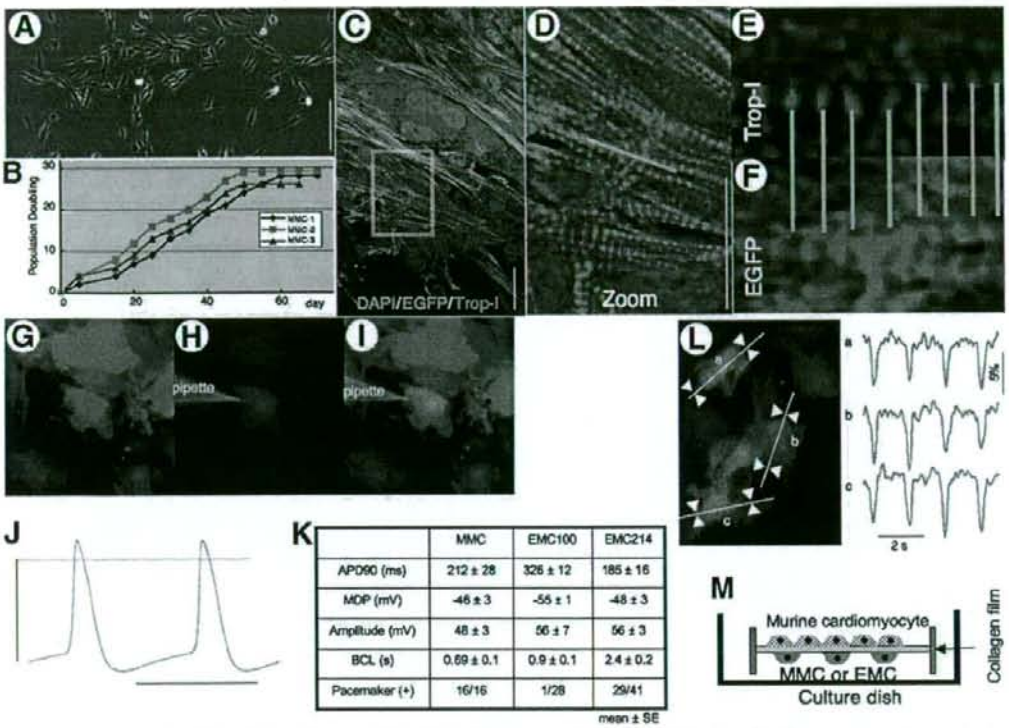

	MMC	EMC100	EMC214
APD90 (ms)	212 ± 28	326 ± 12	185 ± 16
MDP (mV)	-46 ± 3	-55 ± 1	-48 ± 3
Amplitude (mV)	48 ± 3	56 ± 7	56 ± 3
BCL (s)	0.69 ± 0.1	0.9 ± 0.1	2.4 ± 0.2
Pacemaker (+)	16/16	1/28	29/41

mean ± SE

Figure 1. Cardiomyogenic differentiation of menstrual blood-derived mesenchymal cells (MMCs) in vitro. **(A):** Phase-contrast microscopic view of MMC (bar denotes 100 μm), regarded as being PD1, or day 2. **(B):** The representative growth curves of MMCs as a function of time after the culture. The growth curves from all three donors are linear over at least 25 population doublings. **(C–F):** Laser confocal microscopic view of immunocytochemistry of differentiated MMCs with anti-cardiac troponin-I (Trop-I) antibody. Enhanced green fluorescent protein (EGFP)-positive (green) human MMCs expressed Trop-I (red). Scale bar denotes 20 μm. **(D):** Expansion of area within the white box in **(C)**. Clear striation pattern of Trop-I is observed. Trop-I and EGFP images along the yellow line are shown in **(E, F)**. **(E, F):** Trop-I and EGFP staining was observed alternately in striated manner, suggesting Trop-I is expressed in the EGFP-positive cell. **(G–I):** EGFP-labeled MMCs were injected with Alexa 568 solution (red) through a microelectrode to confirm that the recorded signal was obtained from MMCs. **(J):** Representative action potential traces are shown (horizontal line denotes 500 ms). The vertical line denotes 50 mV, and dotted horizontal line denotes 0 mV. **(K):** Action potential parameters. **(L):** A representative still image (left panel) and detected fractional shortening (% FS) along the white line obtained from sites a, b, and c are shown in right panel. **(M):** Experimental schema. Abbreviations: ADP, action potential duration; BCL, basic cycle length; DAPI, 4′-6-diamidino-2-phenylindole; MDP, maximum diastolic potential.

munocytochemistry revealed that the MMCs were stained positive by the anti-cardiac troponin-I antibody (Fig. 1C–1E). Clear striations of red fluorescence of troponin-I in the differentiated MMCs (Fig. 1D, 1E) were observed. Troponin-I and EGFP staining appeared alternately in a striated manner, suggesting troponin-I expressed in the EGFP-positive cell (Fig. 1E, 1F). Clear striations were observed with red fluorescence of α-actinin in the differentiated MMCs (Fig. 2B) and diffuse dot-like staining pattern of connexin 43 around the margin of each EGFP-positive cardiomyocyte (Fig. 2C–2F), suggesting that these human transdifferentiated cardiomyocytes have tight electrical coupling with each other. APs were recorded from spontaneously beating MMCs. The APs obtained from MMCs showed clear cardiomyocyte-specific sustained plateaus and slowly depolarizing resting membrane potentials—so-called "pacemaker potentials" (Fig. 1J, 1K)—and were, therefore, determined to be APs of cardiomyocytes, not of smooth muscle cells, nerve cells, or skeletal muscle cells. The fractional shortening (% FS) of the MMCs was analyzed (Fig. 1L) using a cell edge detection program. The EGFP-positive cells contracted simultaneously within the whole visual field. The % FS was 5.9 ± 0.5% (n = 19).

The percentage of cardiac troponin-I-positive cells was calculated to determine the cardiomyogenic transdifferentiation rate. Whereas MMCs without cocultivation did not show any troponin-I expression (supplemental online Figs. 1A–1D, 2A, 2B), 27%–32% of MMCs became positive for cardiac troponin-I antibody as a result of the cocultivation (Figs. 1C–1F, 4A, supplemental online Fig. 2C, 2D). A cytosine analog, 5-azaC, has a remarkable effect on cell transdifferentiation and has been shown to induce transdifferentiation BMMSCs into cardiomyocytes in mice by nonspecific demethylation of the genome [1]. Cardiomyogenic transdifferentiation was observed in the cocultivated MMCs without any 5-azaC pretreatment, meaning that 5-azaC was not essential for cardiomyogenic transdifferentiation. Nuclear fusion between the cocultivated MMCs and murine cardiomyocytes without separation of the athelocollagen membrane was observed in only 0.16% (3/1846).

Cardiomyogenic Transdifferentiation of EMCs

We hypothesized that the origin of cardiomyogenic cells in the MMCs was the endometrial gland, since MMCs have a high content of detached endometrial glands, whereas circu-

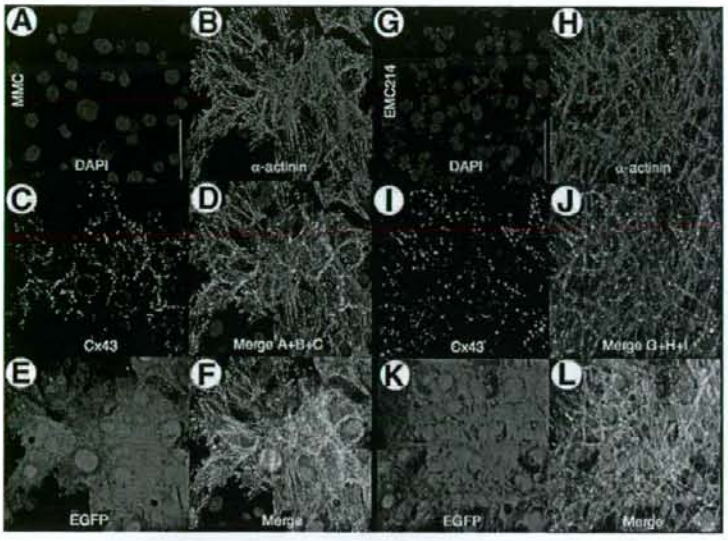

Figure 2. Immunocytochemical analysis of menstrual blood-derived mesenchymal cells (MMCs) and EMC214s stained with anti-sarcomeric α-actinin and connexin 43. **(A–L):** Laser confocal microscopic view of immunocytochemistry of differentiated MMCs and EMC214s with anti-sarcomeric α-actinin (α-actinin) and connexin 43 (Cx43) antibody. **(A–F, G–L):** Enhanced green fluorescent protein (EGFP)-positive (**E, K**; green) human MMCs and EMC214s express α-actinin (**B, H**; red) and Cx43 (**C, I**; cyan). Nuclei are stained with 4′-6-diamidino-2-phenylindole (DAPI) (**A, G**; blue). Clear striation patterns of α-actinin and diffuse Cx43 dot-like staining around the margin of the MMCs and EMC214s were observed. Scale bars in the figure denote 50 μm.

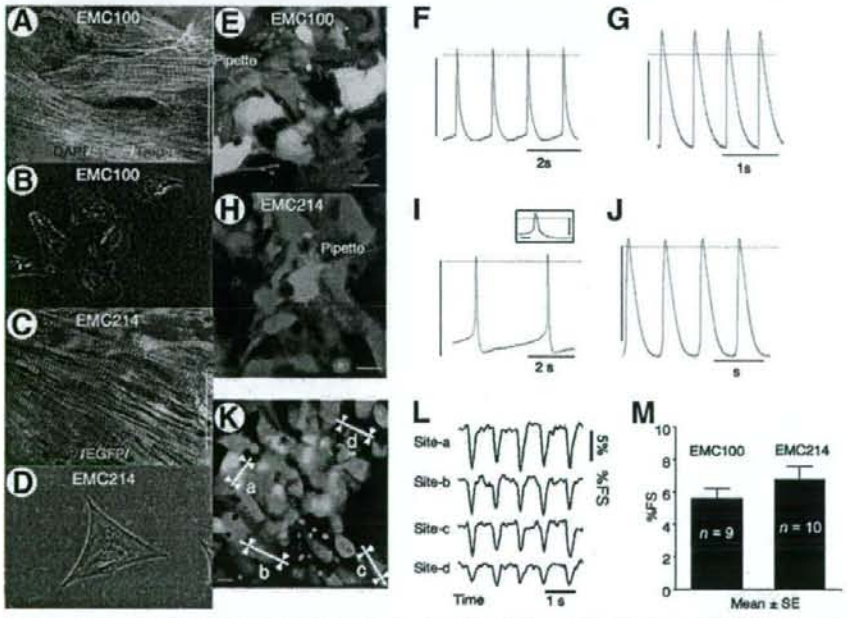

Figure 3. Cardiomyogenic differentiation of endometrial gland-derived mesenchymal cells (EMCs) in vitro. **(A, C):** Immunocytochemistry of differentiated EMC100s (**A**) and EMC214s (**C**) with anti-cardiac troponin-I (Trop-I) antibody. The cells were stained with 4′-6-diamidino-2-phenylindole (DAPI; blue), and anti-cardiac troponin-I antibody (red). Enhanced green fluorescent protein (EGFP)-positive (green) human EMCs expressed Trop-I (red). Please note clear striation staining pattern of Trop-I (**A, C**) in EMCs. Scale bar denotes 20 μm. **(B, D):** Phase-contrast images of EMC100s (**B**) and EMC214s (**D**) before the cardiomyogenic induction. **(E, H):** EGFP-labeled EMC100s and EMC214s (green) were injected with Alexa 568 solution (red) through a microelectrode (**E, H**), and a recorded signal was obtained from the cells. Representative action potential traces are shown (**F, G**: EMC100; **I, J**: EMC214). Action potential of E is expanded in the inset (the vertical line denotes 100 ms). The vertical line denotes 50 mV and dotted horizontal line denotes 0 mV levels. **(K–M):** A representative still image (**K**) and detected fractional shortening (% FS) along the white line obtained from sites a, b, c, and d in (**L**) are shown in (**M**). **(M):** The measured % FS was averaged and is shown.

lating blood-derived endothelial progenitor cells [21] or marrow-derived MSCs [2] do not have such high cardiomyogenic differentiation ability. We consequently established a line of EMCs (Fig. 3B, 3D) with a lifespan prolonged by a cell cycle-mediated gene to ensure a supply of cells for analysis. Almost all EMCs beat strongly in a synchronized manner

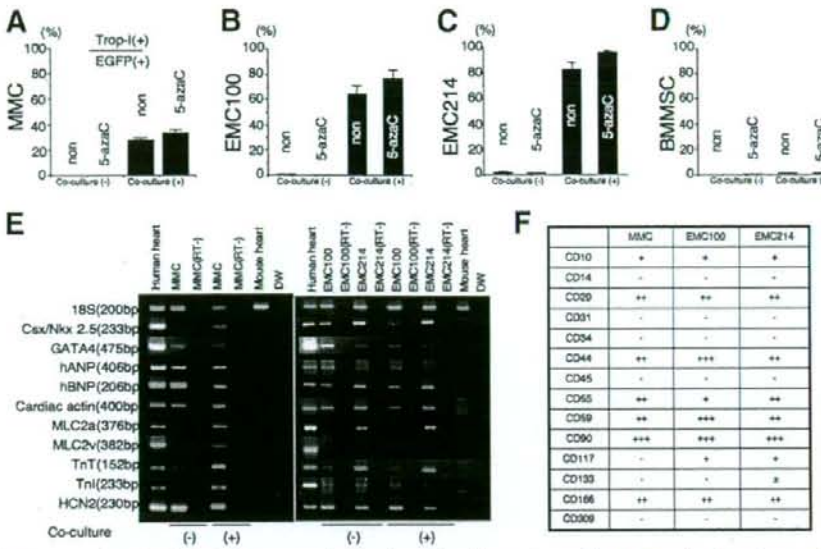

	MMC	EMC100	EMC214
CD10	+	+	+
CD14	-	-	-
CD29	++	++	++
CD31	-	-	-
CD34	-	-	-
CD44	++	+++	++
CD45	-	-	-
CD55	++	+	++
CD59	++	+++	++
CD90	+++	+++	+++
CD117	-	+	+
CD133	-	-	±
CD166	++	++	++
CD309	-	-	-

Figure 4. Cardiomyogenic transdifferentiation rates and expression of cardiomyocyte-specific genes and cell surface markers of menstrual blood-derived mesenchymal cells (MMCs) and endometrial gland-derived mesenchymal cells (EMCs). **(A–D):** Cardiomyogenic transdifferentiation rates of MMCs, EMCs, and bone marrow-derived mesenchymal stem cells (BMMSCs). The character in each column denotes pretreatment with 5-azacytidine (5-azaC) or the lack of treatment (non). **(E):** Reverse transcriptase polymerase chain reaction (PCR) was performed with PCR primers with specificity for human genes encoding cardiac proteins but not for the corresponding murine genes (supplemental online Table 1). Human heart and mouse heart cells were used as a positive control and negative control, respectively. Most human cardiac genes were constitutively expressed in the default state of MMCs and EMCs. **(F):** Summary of flow cytometric analysis of MMCs and EMCs with fluorescein isothiocyanate–coupled antibodies against human surface antigens. Abbreviations: DW, distilled water; EGFP, enhanced green fluorescent protein; hANP, human atrial natriuretic peptide; hBNP, human brain natriuretic peptide; HCN2, cyclic nucleotide-gated potassium channel 2; MLC2a, myosin light chain 2a; MLC2V, myosin light chain 2v; TnI, Trop-I, cardiac troponin I; TnT, cardiac troponin T.

(supplemental online Video 1), and 76.4%–96.5% became positive for cardiac troponin-I antibody as a result of cocultivation (Figs. 3A, 3C, 4B, 4C, supplemental online Fig. 2E–2L). EMCs were also positive for sarcomeric α-actinin and connexin 43 (Fig. 2G–2L). APs were recorded from EMCs. The APs obtained from EMCs showed clear cardiomyocyte-specific sustained plateaus and, in some cells, pacemaker potentials (Fig. 3E–3J). The EGFP-positive EMCs contracted simultaneously within the whole visual field (Fig. 3L, 3M). Nuclear fusion between the cocultivated EMC100s or EMC214s and murine cardiomyocytes without separation of the athelocollagen membrane was observed in only 0.57% (6/1058) or 0.28% (5/1758), respectively.

Expression of Cardiomyocyte-Specific Genes and Surface Markers of EMCs and MMCs

The RT-PCR was performed with primers that hybridized with human cardiomyocyte-specific genes but not with the murine orthologs. Differentiated MMCs and EMCs expressed cardiac-specific genes (Fig. 4D). Interestingly, most of the analyzed genes were expressed in the cells before the induction of transdifferentiation by cocultivation.

There is no difference between surface markers of the MMCs and EMCs. Both cells were positive for CD29 (integrin β1), CD59, and negative for CD14, CD34, CD45, CD309 (Flk-1), etc. (Fig. 4E, supplemental online Fig. 3A–3C).

Cardiomyogenic Effects In Vivo

An EGFP-labeled EMC tissue graft made by a novel 3-dimensional cell sheet manipulation [18] was transplanted into male F344 nude rats to ensure in vivo cardiomyogenic transdifferentiation ability. The EGFP-positive cell layer (green) was observed at the epicardial surface of the host heart (Fig. 5B–5D). Whole EMCs throughout the layer expressed a clear striation staining pattern of sarcomeric α-actinin (Fig. 5B–5G), suggesting extremely high cardiomyogenic transdifferentiation ability of EMCs in situ.

MMCs or BMMSCs were transplanted into the nude rats with MI in vivo. Echocardiography showed that the left ventricular fractional shortening (% LVFS) in the MI+MMC group was significantly greater than it in the MI+BMMSC group at 2 weeks after transplantation (Fig. 6A–6I, supplemental online Fig. 4). The MI area was digitized and every 1-mm depth of tissue section stained with Masson's trichrome (Fig. 6J–6O); averaged data are shown in Figure 6P. The MI area was significantly lower in the MI+MMC group than in the MI+BMMSC group. The EGFP-positive mass of MMCs observed in the MI area expressed a clear striation staining pattern of cardiac troponin-I (Fig. 7) and sarcomeric α-actinin (supplemental online Fig. 5), suggesting an extremely high in situ cardiomyogenic transdifferentiation ability of MMCs, which contributed to improvement in cardiac function.

DISCUSSION

Mechanisms of Highly Cardiomyogenic Transdifferentiation Ability of MMCs and EMCs

The gene expression pattern of MMCs and EMCs before cardiomyogenic transdifferentiation is quite different from that of marrow-derived MSCs [2]. GATA-4 expression in the MMCs and EMCs, and Csx/Nkx 2.5 expression in EMCs with the

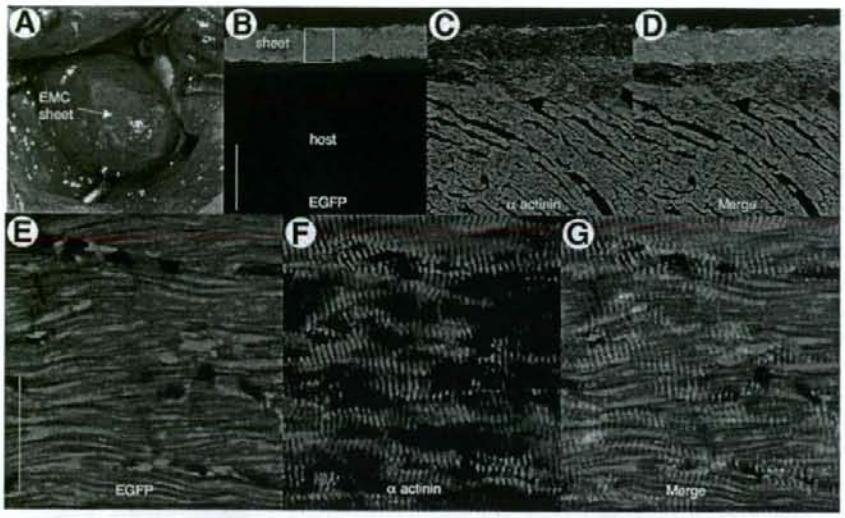

Figure 5. In vivo cardiomyogenesis of endometrium-derived mesenchymal cells (EMCs) in cell sheet tissue graft on host heart. **(A):** Macroscopic view of enhanced green fluorescent protein (EGFP)-labeled EMC tissue graft (sheet) on the epicardial surface of the recipient's heart. **(B–D):** Two weeks after transplantation, immunohistochemistry revealed survival of EMC tissue layer (green) on the recipient heart. Scale bar denotes 100 μm. **(C):** Engrafted EMCs stained positive with anti-sarcomeric α-actinin (red; α-actinin). **(E–G):** The area in the white box in **(B)** is shown in greater detail in **(E–G)**. **(F):** The clear striation pattern of α-actinin staining was observed throughout the entire layer of engrafted EMCs, suggesting extremely high cardiomyogenic potential of EMCs in situ. Scale bar denotes 20 μm.

ability of self-renewal suggest that MMCs and EMCs both have cardiogenic potential and may be termed "cardiac precursor cells" due to their biological features. Cardiac mRNA but not cardiac protein (i.e., troponin-I) was expressed at the default state in the present study, suggesting that both genetic and epigenetic factors may be essential to cause physiologically functioning cardiomyogenic differentiation in MMCs and EMCs. The mechanism of the drastic improvement in the transdifferentiation rate of MMCs and EMCs may be attributable to the default characteristics (expression level of cardiomyocyte-specific mRNA) of MMCs and EMCs in culture compared to marrow-derived MSCs. Highest cardiomyogenic transdifferentiation efficiency was observed in EMC214s (96.5%), EMC100s (76.4%), UCBMSCs (44.9%) [11], MMCs (33.2%), PCPCs (15.1%) [12], and BMMSCs (0.3%, Fig. 4D) [2] in that order. In the practical point of view, EMCs and UCBMSCs are difficult to obtain in enough numbers during the first few passages. MMCs are, therefore, the most suitable cellular source for cardiac stem cell therapy, having a high cardiomyogenic transdifferentiation efficiency. MMCs, EMCs, UCBMSC, and PCPCs are derived from the organ that is related to the pregnancy, therefore the high cardiomyogenic transdifferentiation ability of mesenchymal cells may be caused by a pregnancy-related environmental condition.

Origin of the MMCs and EMCs

Cell surface marker analysis revealed that MMCs are neither encirculating endothelial progenitor cells [22] nor macrophages, but are mesenchymal phenotype cells. We speculated that MMCs may originate in uterine endometrial glands since a lot of detached endometrial glands were observed in menstrual blood and EMCs have the same surface marker as the MMCs, as well as an extremely high cardiomyogenic potential (76.4%–96.5% and 33.2%, respectively). As has been reported, MSCs cannot be detected in circulating blood and all tissues have MSC reservoirs localized in the perivascular niche [23], so EMCs and MMCs do not seem to originate from BMMSCs.

Clinical Contribution

In the present study, MMC transplantation improved impaired cardiac function in vivo. Since MMCs were transplanted at 2 weeks after coronary occlusion, when myocardial necrosis had been completed, the improvement of cardiac function is not due only to transplanted MMC-induced neovascularization [7, 8] or an antiapoptotic [9] effect on infarcted cardiomyocytes. Since they display high cardiomyogenic transdifferentiation ability in vitro and massive cardiomyogenic transdifferentiation in vivo, MMC-derived cardiomyocytes may play a role in the improvement of cardiac function in the present study. Myocardial infarction is known to suppress contraction ability of cardiomyocytes even at normal zone by left ventricular remodeling. Therefore MMC-derived paracrine factors may also play an important role in recovery of % LVFS by prevention of development of LV remodeling.

Neovascularization and the antiapoptotic effect are important for improving cardiac function to some extent. However, the feasible effect is dependent on the number of residual host cardiomyocytes in the infarcted myocardium. To achieve further improvement of cardiac function, a stem cell source that can be expected to exhibit powerful cardiomyogenic transdifferentiation in situ is required. MMCs can be transdifferentiated into cardiomyocytes in situ on the recipient heart, suggesting that they are a promising source for cardiac stem cell-based therapy material, significantly more efficient for cardiomyogenesis than BMMSCs.

MMCs can be readily obtained in a noninvasive manner from young female volunteers, and stored. It should therefore be possible to obtain MMCs of all the HLA types, possibly enabling the establishment of an MMC bank system to facilitate cardiac stem cell-based therapy.

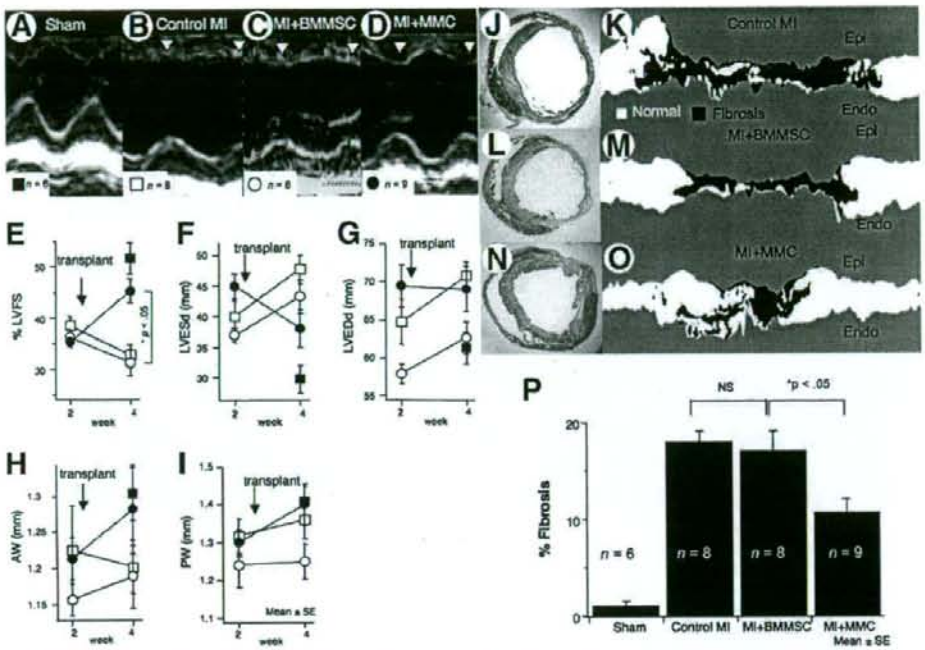

Figure 6. The effect of menstrual blood-derived mesenchymal cell (MMC) transplantation on cardiac function. **(A–D):** Representative M-mode echocardiographic images. The contraction of the left ventricular (LV) anterior wall was improved by transplantation of MMCs (white arrows). The symbol of and number in each group is depicted at the bottom left of each image. **(E–I):** Measured LV parameters are averaged and shown at 2 weeks and 4 weeks after the myocardial infarction (MI). The significant improvement of **(F)** LV end-systolic diameter (LVESd) and **(E)** % fractional shortening (% LVFS) were observed. The diameter of **(H)** anterior left ventricular wall thickness (AW), and **(I)** posterior left ventricular wall thickness (PW). There is no statistical significance. **(J–O):** Representative Masson's trichrome stain images **(J, L, N)** and digitized images **(K, M, O)** of control MI group, MI+bone marrow-derived mesenchymal stem cell (BMMSC), and MI+MMC group are shown. **(P):** The calculated % fibrosis areas are summed and averaged. The MMC transplantation showed significant reduction of % fibrosis area. Abbreviations: Endo, endocardium; Epi, epicardium; NS, not significant.

Role of Established Cardiomyogenic EMC Cell Line for Determining Cardiomyogenic Factors

Several stem cell types are used for clinical patients. Of these, MSCs are reported to show cardiomyogenesis in vitro. Thus, the analysis of key mechanisms for cardiomyogenic differentiation in the human mesenchymal cell is extremely important in order to expand the efficacy of current cardiac stem cell therapy. However, it is very difficult to specify the key factor of cardiomyogenesis by in vivo experiment only. Establishment of EMCs and an in vitro cardiomyogenic differentiation assay system are essential. Stable and high cardiomyogenic transdifferentiation ability in our established system enables us to observe, with wide dynamic range, the effects of treatment for cardiomyogenesis. Moreover, the primary culture condition of murine cardiomyocytes usually fluctuates due to variations in environments, the skill of individual researchers, and institutional differences in isolation protocols. Our established EMCs may provide a good positive control for a cardiomyogenic assay system in vitro to check whether the feeder cell condition is suitable for cardiomyogenic assay. When feeder conditions are suitable, we can survey for possible cardiomyogenic assistant factors or appropriate culture conditions for human BMMSCs by applying various agents or modifying culture conditions systematically. Thus, by using our EMCs and cocultivation system, we may be able to expand the cardiomyogenic differentiation potential of marrow-derived MSCs. Consequently, we may be able to increase the efficacy of cardiac stem cell-based therapy dramatically.

Neither passive stretching of EMCs nor an application of the supernatant of murine cardiomyocyte culture medium to the EMCs alone caused cardiomyocyte differentiation. Taking these findings into account, the multiple environmental factors, including mechanical stretching and/or feeder cardiomyocyte-derived humoral factors, seem to contribute to cardiomyogenic transdifferentiation in human mesenchymal cells. Further experiments should be done.

Study Limitations

Cell fusion between the human cells (MMCs or EMCs) might be a major cause of EGFP-positive cardiomyocytes in the present study. However, EGFP-positive cardiomyocytes could be observed, even when human cells and murine cardiomyocytes were cocultured separately by the athelocollagen membrane that is permeable for only small molecules (less than 5,000 MW)—thus allowing no possible penetration of cells or organelles through the membrane (supplemental online Fig. 6). Furthermore, even if the cells were cocultured without the athelocollagen membrane, nuclear fusion between EMC100s, EMC214s, or MMCs and fetal murine cardiomyocytes was less than 1% in the present study. Moreover, transdifferentiated EMCs at the external layer of the cell sheet graft on the epicardial surface did not directly contact the host cardiomyocytes (Fig. 5). Taking these results

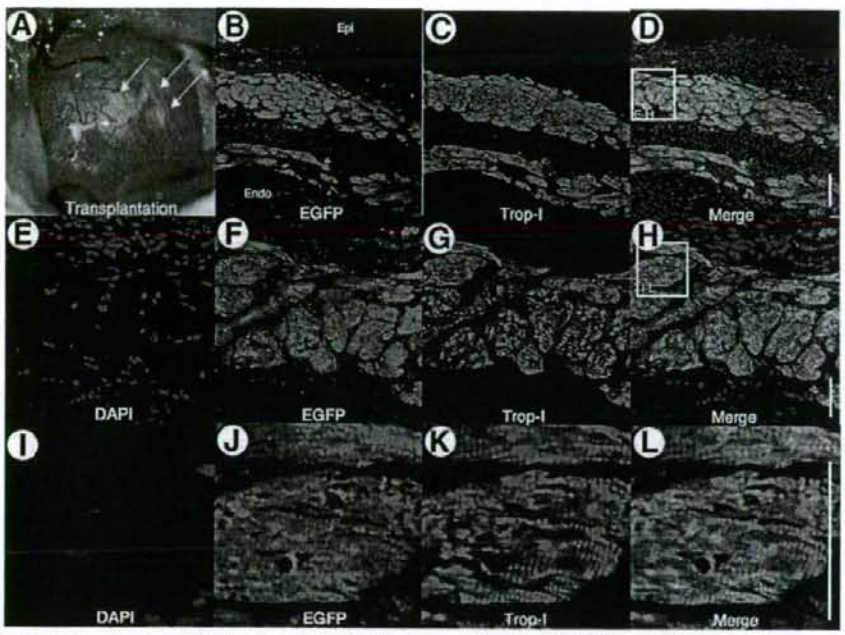

Figure 7. Cardiomyogenesis of engrafted menstrual blood-derived mesenchymal cells (MMCs) in vivo. **(A):** Macroscopic view of the recipient's heart immediately after enhanced green fluorescent protein (EGFP)-labeled MMC transplantation (white arrows) into the myocardial infarction area of the recipient's heart. **(B–L):** Two weeks after transplantation, immunohistochemistry revealed survival of the MMC tissue layer (green) on the treated heart. **(B–D):** Engrafted MMCs stained positive with anti-cardiac troponin-I (red; Trop-1). Scale bar denotes 100 μm. **(E–H, I–L):** The area in the white box in **(D)** was observed in higher resolution **(E–H)** and the white box in **(H)** was also observed in higher resolution **(I–L). (K):** The clear striation pattern of Trop-1 staining was observed throughout the whole layer of engrafted MMCs, suggesting extremely high cardiomyogenic potential of MMCs in situ. Scale bar denotes 20 μm. Abbreviations: DAPI, 4′-6-diamidino-2-phenylindole; Endo, endocardium; Epi, epicardium.

into account, we concluded that the cell fusion did not play a major role in the observed significant cardiomyogenic potential of MMCs and EMCs in the present study.

Infarcted heart tissue may increase auto-fluorescence in some fixative conditions and such auto-fluorescence of host cardiomyocytes might be confused as EGFP-positive like cells. However, autofluorescence of the host myocardium adjacent to the infarcted area was not significant in our present condition (Figs. 5B, 6B, supplemental online Fig. 5B, 5F). Therefore, EGFP-positive tissue in the present study can be defined as of human cell origin and easily distinguished from the host heart by the EGFP fluorescent intensity.

The transfection of the cell cycle-mediated gene may increase cardiomyogenic differentiation to some extent. However, our previous study in human BMMSCs, [2] with the same combination of cell cycle-mediated gene transfection, did not show any increase in efficiency. Furthermore, non-gene-transfected MMCs have an extremely high cardiomyogenic efficiency compared to gene-transfected BMMSCs. Taking these results into account, we concluded that transfection of those genes does not play an essential role in causing such high cardiomyogenic differentiation efficiency in EMCs.

In comparison to previous papers, there was no observable effect of BMMSC transplantation on cardiac function in the present study. This discrepancy may be caused by different experimental conditions, that is, species difference between BMMSCs and the host animal [24], transplantation at acute myocardial infarction [25–27], and usage of immunosuppressive agents, etc [24–27].

In the present study, we did not use a pressure-tipped catheter, therefore the LV dp/dt value may be underestimated.

SUMMARY

MMC transplantation decreased fibrosis area and restored the LV systolic function in the MI-model in vivo. Engrafted MMC transdifferentiated into cardiomyocyte within MI area. MMC can be a major cell source for stem cell therapy to achieve cardiomyogenesis.

ACKNOWLEDGMENTS

The research of N.H. and N.N. was partially supported by a grant from the Ministry of Education, Science and Culture, Japan. A part of this work was undertaken at the Keio Integrated Medical Research Center. We thank M. Uchiyama, A. Furuta, K. Hayakawa, and K. Okamoto for help during the experiments. N.H. and N.N. contributed equally to this work. A part of this work was reported at the annual meeting of the American College of Cardiology 2005, 2006, and 2007.

DISCLOSURE OF POTENTIAL CONFLICTS OF INTEREST

The authors indicate no potential conflicts of interest.

REFERENCES

1 Makino S, Fukuda K, Miyoshi S et al. Cardiomyocytes can be generated from marrow stromal cells in vitro. J Clin Invest 1999;103:697–705.
2 Takeda Y, Mori T, Imabayashi H et al. Can the life span of human marrow stromal cells be prolonged by bmi-1, E6, E7, and/or telomerase without affecting cardiomyogenic differentiation? J Gene Med 2004;6: 833–845.
3 Chen SL, Fang WW, Ye F et al. Effect on left ventricular function of intracoronary transplantation of autologous bone marrow mesenchymal stem cell in patients with acute myocardial infarction. Am J Cardiol 2004;94:92–95.
4 Orlic D, Kajstura J, Chimenti S et al. Bone marrow cells regenerate infarcted myocardium. Nature 2001;410:701–705.
5 Wang JS, Shum-Tim D, Galipeau J et al. Marrow stromal cells for cellular cardiomyoplasty: Feasibility and potential clinical advantages. J Thorac Cardiovasc Surg 2000;120:999–1005.
6 Shake JG, Gruber PJ, Baumgartner WA et al. Mesenchymal stem cell implantation in a swine myocardial infarct model: Engraftment and functional effects. Ann Thorac Surg 2002;73:1919–1926.
7 Gojo S, Gojo N, Takeda Y et al. In vivo cardiovasculogenesis by direct injection of isolated adult mesenchymal stem cells. Exp Cell Res 2003; 288:51–59.
8 Tang YL, Zhao Q, Zhang YC et al. Autologous mesenchymal stem cell transplantation induce VEGF and neovascularization in ischemic myocardium. Regul Pept 2004;117:3–10.
9 Gnecchi M, He H, Liang O et al. Paracrine action accounts for marked protection of ischemic heart by Akt-modified mesenchymal stem cells. Nat Med 2005;11:367–368.
10 Kocher AA, Schuster MD, Szabolcs MJ et al. Neovascularization of ischemic myocardium by human bone-marrow-derived angioblasts prevents cardiomyocyte apoptosis, reduces remodeling and improves cardiac function. Nat Med 2001;7:430–436.
11 Nishiyama N, Miyoshi S, Hida N et al. The significant cardiomyogenic potential of human umbilical cord blood-derived mesenchymal stem cells in vitro. STEM CELLS 2007;25:2017–2024.
12 Okamoto K, Miyoshi S, Toyoda M et al. 'Working' cardiomyocytes exhibiting plateau action potentials from human placenta-derived extraembryonic mesodermal cells. Exp Cell Res 2007;313:2550–2562.
13 Terai M, Uyama T, Sugiki T et al. Immortalization of human fetal cells: the life span of umbilical cord blood-derived cells can be prolonged without manipulating p16INK4a/RB braking pathway. Mol Biol Cell 2005;16:1491–1499.
14 Takeuchi M, Takeuchi K, Kohara A et al. Chromosomal instability in human mesenchymal stem cells immortalized with human papilloma virus E6, E7, and Htert genes. In Vitro Cell Dev Biol Anim 2007;43: 129–138.
15 Schwab KE, Gargett CE. Co-expression of two perivascular cell markers isolates mesenchymal stem-like cells from human endometrium. Hum Reprod 2007;22:2903–2911.
16 Meng X, Ichim TE, Zhong J et al. Endometrial regenerative cells: A novel stem cell population. J Transl Med 2007;5:57–66.
17 Kyo S, Nakamura M, Kiyono T et al. Successful immortalization of endometrial glandular cells with normal structural and functional characteristics. Am J Pathol 2003;163:2259–2269.
18 Itabashi Y, Miyoshi S, Kawaguchi H et al. A new method for manufacturing cardiac cell sheets using fibrin-coated dishes and its electrophysiological studies by optical mapping. Artificial Organs 2004;29:95–103.
19 Furuta A, Miyoshi S, Itabashi Y et al. Pulsatile cardiac tissue grafts using a novel three-dimensional cell sheet manipulation technique functionally integrates with the host heart, in vivo. Circ Res 2006;98:705–712.
20 Iijima Y, Nagai T, Mizukami M et al. Beating is necessary for transdifferentiation of skeletal muscle-derived cells into cardiomyocytes. FASEB J 2003;17:1361–1363.
21 Koyanagi M, Urbich C, Chavakis E et al. Differentiation of circulating endothelial progenitor cells to a cardiomyogenic phenotype depends on E-cadherin. FEBS Lett 2005;579:6060–6066.
22 Asahara T, Murohara T, Sullivan A et al. Isolation of putative progenitor endothelial cells for angiogenesis. Science 1997;275:964–967.
23 da Silva Meirelles L, Chagastelles PC, Nardi NB. Mesenchymal stem cells reside in virtually all post-natal organs and tissues. J Cell Sci 2006;119:2204–2213.
24 Wang JA, Fan YQ, Li CL et al. Human bone marrow-derived mesenchymal stem cells transplanted into damaged rabbit heart to improve heart function. J Zhejiang Univ Sci B 2005;6:242–248.
25 Zhang S, Ge J, Sun A et al. Comparison of various kinds of bone marrow stem cells for the repair of infarcted myocardium: Single clonally purified non-hematopoietic mesenchymal stem cells serve as a superior source. J Cell Biochem 2006;99:1132–1147.
26 Grauss RW, Winter EM, van Tuyn J et al. Mesenchymal stem cells from ischemic heart disease patients improve left ventricular function after acute myocardial infarction. Am J Physiol Heart Circ Physiol 2007;293: H2438–H2447.
27 Hou M, Yang KM, Zhang H et al. Transplantation of mesenchymal stem cells from human bone marrow improves damaged heart function in rats. Int J Cardiol 2007;115:220–228.

See www.StemCells.com for supplemental material available online.

Novel Cardiac Precursor-Like Cells from Human Menstrual Blood-Derived Mesenchymal Cells

Naoko Hida, Nobuhiro Nishiyama, Shunichiro Miyoshi, Shinichiro Kira, Kaoru Segawa, Taro Uyama, Taisuke Mori, Kenji Miyado, Yukinori Ikegami, ChangHao Cui, Tohru Kiyono, Satoru Kyo, Tatsuya Shimizu, Teruo Okano, Michiie Sakamoto, Satoshi Ogawa and Akihiro Umezawa

Stem Cells 2008;26;1695-1704; originally published online Apr 17, 2008;
DOI: 10.1634/stemcells.2007-0826

日程	班	氏名	テーマ	プレゼンテーション(60)	レポート(15)	質疑(10)	出席(15)	質問(5)	時間	合計
		青山剛三		58		5	15	5		83
		阿部舞美		60	15	7	15	5		102
		池永有里		57	15	7	15	5		99
		上村怜央		58	15	8	15	5		101
		浦上信太郎		60	15	10	15	5		105
		岡村真弥		60	15	10	15	5		105
		奥村美帆		60	15	10	15	5		105
		川口明日香		60	15	10	15	5		105
		川口佳保理		55	15	10	15	5		100
		川崎友美		55	15	7	7	5		89
		黒田景子		58	15	10	15	5		103
		後藤祐美		60	15	7	15	5		102
		小林友幸		60	15	8	15	5		103
		酒井博生		57	15	7	15	5		99
		清水友理		58	15	8	15	5		101
		社領美紀		60	15	10	15	5		105
		須河内昭成		60	15	10	15	5		105
		千田百合絵		60		8	15	5		88
		西原千尋		50	15	5	15	5		90

A 歯周疾患と骨
B 破骨細胞と骨吸収の調節メカニズム
C 遺伝子と歯周疾患
D 骨芽細胞と骨形成の調節メカニズム
E 骨リモデリング
F 遺伝子と歯科疾患
G 歯と歯周組織の再生について
H 細胞外マトリックス

Establishment of an immortalized human extravillous trophoblast cell line by retroviral infection of E6/E7/hTERT and its transcriptional profile during hypoxia and reoxygenation

HIROKO OMI[1], AIKOU OKAMOTO[1,2], TAKASHI NIKAIDO[3], MITSUYOSHI URASHIMA[4], RIE KAWAGUCHI[1], NAGAYOSHI UMEHARA[1], KENTARO SUGIURA[1], MISATO SAITO[1], TOHRU KIYONO[5] and TADAO TANAKA[1]

Departments of [1]Obstetrics and Gynecology, [2]Gene Therapy, Institute of DNA Medicine, [3]Department of Pathology, [4]Division of Clinical Research and Development, The Jikei University, School of Medicine, 3-25-8 Nishishinbashi, Minato-ku, Tokyo 105-8461; [5]Virology Division, National Cancer Center Research Institute, 5-1-1 Tsukiji, Chuo-ku, Tokyo 104-045, Japan

Received September 26, 2008; Accepted October 29, 2008

DOI: 10.3892/ijmm_00000121

Abstract. Investigation into the function of human trophoblasts has been largely restricted by a lack of suitable cell models. We aimed to produce normal human trophoblast cell lines with a long lifespan and to provide an ideal *in vitro* cell model. Primary human trophoblast cells were derived from a placenta that had undergone elective abortion at the 7th week of gestation. The cells were immortalized by infection with retroviral expression vectors containing the type 16 human papillomaviruses E6 and E7 in combination with human telomerase reverse transcriptase (hTERT). Characterization of the cell line was performed by immunocytochemistry using a panel of antibodies, Western blotting, real-time RT-PCR, an invasion assay, gelatin zymography, karyotype analysis and a nude mouse assay. Gene expression profiles under hypoxia (1% O_2, 1 h) and subsequent reoxygenation (20% O_2, 6 h) were analyzed using cDNA microarray. Immunocytochemistry revealed an extravillous trophoblastic phenotype by positive staining for hCGß, cytokeratin 7, HLA-G and CD9. A transwell insert invasion assay showed the invasiveness of this cell line and gelatin zymography detected the secretion of MMP-2 and MMP-9. Karyotype analysis exhibited an almost normal chromosomal number which ranged from 46 to 48 and the cells showed no tumorigenecity in a nude mouse assay. Forty-three genes showing reversible up- or down-regulation during hypoxia were detected using an oligonucleotide array. This newly immortalized cell line, HChEpC1b, is a useful model for the study of extravillous trophoblast function.

Correspondence to: Dr Tadao Tanaka, Department of Obstetrics and Gynecology, The Jikei University, School of Medicine, 3-25-8 Nishishinbashi, Minato-ku, Tokyo 105-8461, Japan
E-mail: tanaka3520@jikei.ac.jp

Key words: trophoblast, immortalization, human papillomavirus, E6, E7, human telomerase reverse transcriptase, hypoxia, oligonucleotide microarray

Introduction

In humans, cells outside the morula form the trophoectoderm and differentiate into trophoblasts. These cells form the fetal compartment of the placenta during pregnancy. After the initial phase of implantation, human trophoblasts differentiate along either the villous or the extravillous trophoblast pathway. Multinucleate syncytiotrophoblasts, which form the epithelial layer of the villi by cell fusion, are involved in the exchange of gas and the nutrients between the mother and the fetus. Mononuclear extravillous cytotrophoblasts invade deep into the decidua, the myometrium and the uterine spiral arteries (1). Clinically, many pregnancy-associated conditions result from abnormal functioning of trophoblasts, such as abortion, intrauterine growth retardation and pre-eclampsia (2).

Investigation into the function of human trophoblasts has been largely restricted by the short life span of primary cultured trophoblasts *in vitro*. There are two major mechanisms that cause the limited life span of primary cultured cells. One is the telomere-based replication senescence (3,4) and the other is telomere-independent senescence, which is thought to be controlled by the Rb/p16 (5) and p53 pathways (6). Since HPV16 E6/and E7 are known to inhibit p53 and Rb function, respectively, we introduced E6/E7 and human telomerase reverse transcriptase (hTERT) into primary human trophoblast cells to immortalize them.

We obtained one cell line, HChEpC1b, that retained an extravillous phenotype and acquired immortality. This cell line expressed molecular markers for human extravillous trophoblasts and it demonstrated invasiveness and metalloproteinase production; nevertheless, it did not show tumorigenic potency. There have been a number of trophoblast cell lines that have gained a long life span spontaneously (7-12), or by transduction of the SV40 T antigen (7,13-17), HPV16 E6/E7 (18,19) and hTERT (20). However, this is the

first study of an immortalized trophoblast cell line produced by retroviral infection of HPV16 E6/E7 in combination with hTERT and this newly established cell line may provide a useful model for the study of extravillous trophoblast function as well as that of other cell lines.

Materials and methods

Preparation of human trophoblast primary cultures. A human placenta was obtained from a patient that had undergone a legal termination of a normal pregnancy at 7 weeks of gestation with informed consent. This study was approved by the Ethics Committee of the Jikei University. After removal of all attached decidual tissue and blood clots, chorionic villi were gently shaken in normal saline solution. The fallen cells and tissue fragments were collected and suspended in RPMI-1640 (Sigma-Aldrich, Tokyo, Japan) supplemented with 10% fetal bovine serum (Invitrogen Corp., Carlsbad, CA, USA), 50 IU/ml penicillin, 50 μg/ml streptomycin, and 100 mg/ml neomycin (Invitrogen Corp) and were cultured in a collagen I coated culture dish (Asahi Techno Glass, Tokyo, Japan). Two weeks later, colonies were collected using cloning rings with 0.05% trypsin and 0.53 mM EDTA (Invitrogen Corp) and were transferred to a 24-well culture dish. When the colonies became confluent, the cells were transferred to a 6-well culture dish. Three clones with epithelioid phenotypes [human chorionic epithelium cell-1 (HChEpC1) a-c] were selected for the next immortalization step.

Vector construction and retroviral transduction of E6/E7 and hTERT. Construction of retroviral vector plamids, pCMSCV puro-hTERT, pCLXSN-16E6E7, has been described previously (21). Production of recombinant retroviruses was carried out, as previously described (22). Briefly, a retroviral vector and packaging construct, pCL-10A1, was co-transduced into 293T cells using TransIT-293 (Mirus Bio Corp., Madison, WI, USA) according to the manufacturer's instructions. The culture fluid was harvested at 48 to 72 h post-transduction. The titer of the recombinant viruses was $>1x10^5$ drug-resistant colony-forming U/ml on HeLa cells. HChEpC1 cells seeded on 24-well dishes were inoculated with a 0.5 ml aliquot of the culture fluid in the presence of polybrene (4 μg/ml). Following inoculation with viruses, the cells were grown without drug selection as mock-infected cells and stopped growing within two weeks. To achieve different combinations of retroviral infections, the cells were serially infected with MSCVpuro-hTERT and LXSN-16E6E7 at passage 2.

Cell culture. The infected HChEpC1 cells were cultured in RPMI-1640 supplemented with 10% FBS, 50 U/ml penicillin G, 50 μg/ml streptomycin, and 100 mg/ml neomycin and were incubated in 5% CO_2 air at 37˚C. Serial passages were made in one to four splits. One clone, HChEpC1b, was selected for further characterization because it had the highest purity of trophoblast cells as proved by its uniformly positive staining for hCGß. The population doubling time (DT) was calculated as follows: $DT = T \times \log_2/\log (N_T/N_0)$, where N_0 is the initial number of cells and N_T is the number of cells harvested after T h culture.

The choriocarcinoma cell lines JAR and JEG-3 and the fibroblast cell line Hs795Pl were obtained from ATCC and propagated in RPMI-1640, MEM (Invitrogen Corp) and DMEM (Invitrogen Corp) respectively, supplemented with 10% FBS.

Karyotyping. Cells in the exponential phase were arrested by adding 0.03 μg/ml of colchicine for 6 h, before being treated with hypotonic solution (75 mM KCl, pH 8.0) and fixed twice in Carnoy's fixative (methanol/acetic acid). The G-band pattern was obtained using Giemsa staining and the chromosomes of 20 metaphases were analyzed.

Nude mouse assay. Single cell suspensions (10^7 cells) of HChEpC1b cells or JAR cells were subcutaneously inoculated into the right flank of 5 female mice (balb/c nu/nu) each. These mice were observed for up to 3 months and examined for tumor growth.

Immunocytochemistry. HChEpC1b cells were cultured on collagen I coated culture slides (BD Biosciences, Bedford, MA, USA) for two days, washed once with phosphate-buffered saline (PBS, pH 7.4) and fixed with 100% ethanol (room temperature) for 30 min. After three 5-min hydration periods in distilled water (room temperature) and two 10-min periods of washing in 0.1% Tween in PBS (4˚C), the cells were incubated overnight at 4˚C with the primary antibodies diluted in Antibody Diluent (Dako, Glostrup, Denmark) as described in Table I. The cells were washed three times with 0.1% Tween in PBS (4˚C) and incubated with EnVision Labelled Polymer, Peroxidase (Dako) for 1 h at room temperature. After washing three times with 0.1% Tween in PBS (4˚C), visualization was developed according to the manufacturer's instructions using diaminobenzidine (DAB) as the substrate. The cells were counterstained with hematoxylin, dehydrated and mounted for light microscopy.

Real-time reverse transcriptase polymerase chain reaction (real-time RT-PCR). Total RNA were isolated from subconfluent cultured cells using the RNeasy mini kit (Qiagen, Gmbh Hilden, Germany). Reverse transcription was performed according to the manufacturer's protocol (Takara RNA PCR kit, Takara, Shiga, Japan) with 1 μg of total RNA. For real-time PCR, each target was amplified on the same plate with GAPDH as the reference using the Taq Man Universal PCR master mix and the ABI PRISM 7700 sequence detection system (Applied Biosystems, Foster City, USA) and the relative mRNA amounts and range were determined. The primer/probe sets were purchased from Taq Man gene expression assays (Applied Biosystems, Assay IDs are listed in Table II). Relative mRNA levels were calculated by the comparative C_T method described in ABI User Bulletin 2.

Western blotting. Subconfluent HChEpC1b, JAR, JEG-3 and Hs795Pl cells were scraped from culture dishes, washed three times with cold PBS, and then incubated in the RIPA buffer [10 mM Tris-HCl (pH 7.5), 150 mM NaCl, 2 mM EDTA, 1% NP-40, 1% sodium deoxycholate, 0.1% SDS, complete mini (Roche, Basel, Switzerland)] for 30 min on ice. After centrifugation, the supernatants were subjected to Western blot

Table I. Antibodies used for immunocytochemistry and Western blotting.

Epitope	Clone name	Host	Isotype	Company	Cat. no.	Nation	Dilution
Cytokeratin 7	OVTL 12-30	Mouse	IgG1 κ	Acris Antibodies	DM057	Germany	1:50
HLA class I	W6/32HL	Mouse	IgG2a	Chemicon International	CBL139	USA	1:50
HLA-G	87G	Mouse	IgG2a	Exbio	10-437-C100	Czech	1:100
HLA-G	MEM-G/1	Mouse	IgG1	Serotec	MCA2043	UK	1:50
CD9	Polyclonal	Rabbit	IgG	Santa Cruz Biotechnology	sc-9148	USA	1:50
CD9	M-L13	Mouse	IgG1 κ	BD Biosciences	555370	USA	1:50
Vimentin	V9	Mouse	IgG1	Chemicon International	MAB3400	USA	1:200
E-cadherin	Polyclonal	Rabbit	IgG	Santa Cruz Biotechnology	sc-7870	USA	1:50
hCG ß	Polyclonal	Rabbit	IgG	Dako	A0231	USA	1:50
hPL	Polyclonal	Rabbit	IgG	Lab Vision	RB-9067-P	UK	1:50
PLAP	8B6	Mouse	IgG2a	Chemicon International	CBL207	USA	1:50

Table II. Details of assay ID for real-time PCR.

Gene	Assay ID
Cytokeratin 7	Hs00818825_m1
HLA-G	Hs00918802_m1
CD9	Hs00233521_m1
HPL	Hs01862611_g1
PLAP	Hs01654626_s1
Vimentin	Hs00185584_m1
Integrin α-1	Hs00235006_m1
Integrin α-6	Hs00173952_m1
Integrin ß-1	Hs00559595_m1
Integrin ß-4	Hs00236216_m1

analysis. Total proteins (20 μg) per sample was electrophoresed on a 4-20% SDS-polyacrylamide gel and transferred to a PDVF membrane. After washing in TBST (0.1% Tween in Tris-buffered saline), the membrane was incubated with primary antibodies (anti-cytokeratin 7, 1:500; anti-E-cadherin, 1:500; anti-vimentin, 1:1000) for 1 h at 37˚C, before being washed in TBST and incubated with secondary HRP-conjugated goat anti mouse or rabbit IgG goat antibodies (Santa Cruz Biotechnology, Santa Cruz, CA, USA) for 1 h at 37˚C. The antigen-antibody complexes were visualized using DAB.

Gelatin zymography. The gelatinolytic activities of matrix metalloproteinase-2 (MMP-2) and MMP-9 were assayed using gelatin zymography. Subconfluent cells were rinsed and cultured with serum-free medium for three days. The harvested medium was mixed 1:1 with 2X sample buffer [125 mM Tris-HCl (pH 6.8), 4% SDS, 20% glycerol] and was then applied to gels for electrophoresis without boiling under nonreducing conditions in a 10% acrylamide gel containing 1 mg/ml gelatin (Invitrogen Corp). After electrophoresis, the gels were washed at room temperature for 1 h in a buffer consisting of 50 mM Tris-HCl (pH 7.5) and 2.5% Triton X-100 to remove SDS and were then incubated overnight in a buffer consisting of 50 mM Tris-HCl (pH 7.6), 150 mM NaCl, 10 mM $CaCl_2$ and 0.05% NaN_3 at 37˚C. The gels were stained with 0.25% Coomassie Brilliant Blue R-250 in 50% methanol and 5% acetic acid for 60 min and destained in 5% methanol and 7% acetic acid. MMP-2 and MMP-9 were visualized as clear bands against a dark background at 72 and 92 kDa, respectively.

In vitro invasion assay. Invasion assays were carried out using BD Matrigel Invasion Chambers, 24-well plate, 8-mm pore size (BD Biosciences). Cells were seeded at a density of 25,000 cells/well in 500 μl culture medium. Following incubation periods of 24 and 48 h, the filter inserts were removed and washed twice with PBS and the upper side of the filter was cleaned with a cotton tipped swab. For assessment of the number of invaded cells, the filters were fixed and stained with 0.2% crystal violet in 4% formaldehyde. The total number of cells that had invaded onto the underside of the filter was counted manually under a light microscope.

Hypoxia-reoxygenation treatment. HChEpC1b cells were incubated under normoxic conditions (20% O_2) and then were subjected to hypoxia (1% O_2) for 1 h and subsequent reoxygenation under normoxic conditions (20% O_2) for 6 h. At the end of each culture period, cells were scraped from culture dishes and were centrifuged and snap-frozen. All samples were stored at -80˚C before analysis and total RNA were isolated using the RNeasy mini kit (Qiagen).

Microarray analysis. Human genome-wide gene expression was examined using the Human Genome U133 Plus 2.0 Array (HG-U133 Plus 2.0 Set: GeneChip, Affymetrix, Santa Clara, CA, USA), which contains almost 45,000 probe sets, representing >39,000 transcripts derived from ~33,000 well-substantiated human genes (http://www.affymetrix.com/products/arrays/specific/hgu133.affx). Double-stranded cDNA was synthesized and the cDNA was subjected to *in vitro* transcription in the presence of biotinylated nucleotide triphosphates. Ten micrograms of the biotinylated cRNA was hybridized with a probe array for 16 h at 45˚C and the